

1 **Less surface sea ice melt in the CESM2 improves Arctic sea ice simulation with minimal**  
2 **non-polar climate impacts**

3  
4  
5 Jennifer E. Kay<sup>1,2</sup>, Patricia DeRepentigny<sup>1,3</sup>, Marika M. Holland<sup>4</sup>, David A. Bailey<sup>4</sup>, Alice K.  
6 DuVivier<sup>4</sup>, Ed Blanchard-Wrigglesworth<sup>5</sup>, Clara Deser<sup>4</sup>, Alexandra Jahn<sup>1,3</sup>, Hansi Singh<sup>6</sup>, Madison  
7 M. Smith<sup>5</sup>, Melinda A. Webster<sup>7</sup>, Jim Edwards<sup>4</sup>, Sun-Seon Lee<sup>8,9</sup>, Keith B. Rodgers<sup>8,9</sup>, and Nan  
8 Rosenbloom<sup>4</sup>

9  
10 <sup>1</sup>Department of Atmospheric and Oceanic Sciences, University of Colorado, Boulder, CO

11 <sup>2</sup>Cooperative Institute for Research in Environmental Science, University of Colorado, Boulder,  
12 CO

13 <sup>3</sup>Institute of Arctic and Alpine Research, University of Colorado, Boulder, CO

14 <sup>4</sup>National Center for Atmospheric Research, Boulder, CO

15 <sup>5</sup>University of Washington, Seattle, WA

16 <sup>6</sup>University of Victoria, British Columbia, Canada

17 <sup>7</sup>University of Alaska Fairbanks, AK

18 <sup>8</sup>Center for Climate Physics, Institute for Basic Science, Busan, South Korea

19 <sup>9</sup>Pusan National University, Busan, South Korea

20  
21 Corresponding author: Jennifer E. Kay (jennifer.e.kay@colorado.edu)

22 Revised for *Journal of Advances in Modeling Earth Systems*

23 November 22, 2021

24  
25 Publication Units: 6603 words (~13 PU, each PU is 500 words), 15 Figures. Total PU = 28.

26  
27 **Key Points:**

- 28
- Decreasing surface melt decreases late-summer Arctic sea ice cover biases and delays  
29 transition to an ice-free Arctic Ocean
  - Internal variability limits value of sea ice trends and sea ice sensitivity as metrics to  
30 constrain model performance under similar global warming
  - Increasing sea ice thickness and area has negligible impacts on non-polar climate and  
31 climate change
- 32  
33

34 **Abstract**

35

36 This study isolates the influence of sea ice mean state on pre-industrial climate and transient  
37 1850-2100 climate change within a fully coupled global model: The Community Earth System  
38 Model version 2 (CESM2). The CESM2 sea ice model physics is modified to increase surface  
39 albedo, reduce surface sea ice melt, and increase Arctic sea ice thickness and late summer cover.  
40 Importantly, increased Arctic sea ice in the modified model reduces a present-day late-summer  
41 ice cover bias. Of interest to coupled model development, this bias reduction is realized without  
42 degrading the global simulation including top-of-atmosphere energy imbalance, surface  
43 temperature, surface precipitation, and major modes of climate variability. The influence of these  
44 sea ice physics changes on transient 1850-2100 climate change is compared within a large initial  
45 condition ensemble framework. Despite similar global warming, the modified model with thicker  
46 Arctic sea ice than CESM2 has a delayed and more realistic transition to a seasonally ice free  
47 Arctic Ocean. Differences in transient climate change between the modified model and CESM2  
48 are challenging to detect due to large internally generated climate variability. In particular, two  
49 common sea ice benchmarks - sea ice sensitivity and sea ice trends - are of limited value for  
50 comparing models with similar global warming. More broadly, these results show the importance  
51 of a reasonable Arctic sea ice mean state when simulating the transition to an ice-free Arctic  
52 Ocean in a warming world. Additionally, this work highlights the importance of large initial  
53 condition ensembles for credible model-to-model and observation-model comparisons.

54

55

56 **Plain Language Summary**

57

58 Satellite observations available from 1979 to present show dramatic Arctic sea ice loss. As a  
59 result, projecting when the Arctic Ocean may become ice free and the resulting impacts is of  
60 broad interest to those living in the Arctic and beyond. Climate models are the main tool for making  
61 such future projections. Yet, projecting sea ice loss is hard because it is affected by multiple  
62 factors that are often impossible to disentangle including physical processes, unpredictable  
63 climate variability, and differences in climate drivers. Unique to this work, we analyze the influence  
64 of the sea ice surface melt while also controlling for all other confounding factors such as the  
65 amount of global warming and unpredictable climate variability. Our work demonstrates that under  
66 similar global warming, surface melt affects the timing of an ice-free Arctic Ocean. Specifically,  
67 simulations with less surface melt and more sea ice transition to an ice-free Arctic Ocean later.  
68 From the perspective of model development and transient climate change, we also found sea ice  
69 amounts and the timing towards an ice-free Arctic have negligible influence on warming,  
70 precipitation, and sea level pressure outside of the polar regions.

## 71 **1. Motivation and Study Goals**

72 Satellite-observed Arctic Ocean sea ice cover decreases over the last few decades are a  
73 visible manifestation of human-caused climate change. Earth system models cannot reproduce  
74 this observed ice loss with natural forcing alone (e.g., Kirchmeier-Young et al. 2017, Kay et al.  
75 2011). While models can reproduce the sign of observed multi-decadal Arctic sea ice area trends,  
76 these same models exhibit differing Arctic sea ice loss rates and timing (Swart et al. 2015, Notz,  
77 D & SIMIP Community 2020). Why do Arctic sea ice loss rates differ between model simulations?  
78 Given similar global warming, two factors are important to consider. First, mean state matters:  
79 models with thicker Arctic sea ice tend to exhibit less ice area loss but more ice volume loss than  
80 models with thinner sea ice (e.g., Massonnet et al. 2018, Holland et al. 2010, Bitz 2008). Second,  
81 internally generated climate variability influences differences in Arctic sea ice loss timing and  
82 trends (e.g., Notz, D & SIMIP Community 2020, England et al. 2019, Jahn et al. 2016, Swart et  
83 al. 2015, Notz 2015, Wettstein and Deser 2014, Kay et al. 2011). In fact, recent work emphasizes  
84 that internal variability dominates over emissions scenario in affecting projected sea ice loss over  
85 the upcoming 2-3 decades, including the timing of the first ice-free Arctic Ocean in late summer  
86 (e.g., Bonan et al., 2021, DeRepentigny et al. 2020, Jahn 2018, Sigmond et al. 2018).

87

88 Sea ice mean state influences transient sea ice response to climate forcing. Indeed, mean  
89 sea ice thickness has well-known foundational influences on vertical sea ice thermodynamics  
90 (Bitz and Roe 2004, Holland et al. 2006). The two dominant feedbacks internal to sea ice – the  
91 positive sea ice albedo feedback and the negative ice-thickness growth feedback – strengthen  
92 when sea ice thins. Sea ice loss in models with a wide range of complexities show the importance  
93 of sea ice mean thickness to thermodynamic sea ice growth and loss. In addition, mean sea ice  
94 thickness affects sea ice variability and predictability. When sea ice thins, ice area variability  
95 increases, ice thickness variability decreases, and predictor relationships change in location,  
96 nature, and magnitude (e.g., Holland et al. 2019, Mioduszewski et al. 2018, Swart et al. 2015,  
97 Holland and Stroeve 2011, Blanchard Wrigglesworth et al. 2011, Kay et al. 2011).

98

99 While the importance of sea ice mean state is uncontroversial, the potential to constrain  
100 the mean state and reduce projection uncertainty remains unclear. Recent work by Massonnet et  
101 al. (2018) used regression to quantify the relationship between Arctic sea ice mean state and  
102 transient loss rates in a multi-model ensemble (Coupled Model Intercomparison Project version  
103 5 (CMIP5), Taylor et al. 2012). While the relationships between mean state and linear changes in  
104 March sea ice volume and September sea ice area were weak, they were statistically significant.

105 The study arrived at two important conclusions. First, given the importance of mean state and in  
106 particular sea ice thickness mean state, models with a biased mean sea ice thickness should be  
107 questioned and potentially not used for future projections. Second, it is currently not possible to  
108 observationally constrain the sea ice thickness mean state due to the lack of long-term and  
109 reliable observations. This second conclusion is especially striking, is consistent with a recent  
110 community analysis that questioned the accuracy of sea ice thickness observations (e.g., Notz,  
111 D. & SIMIP Community 2020), and leaves many open questions: 1) How reliable is reliable  
112 enough? 2) How long of an observational record is needed? 3) Does tuning to observed sea ice  
113 extent/area help constrain sea ice thickness? Model tuning is necessary (e.g., Mauritsen et al.  
114 2012), and best accomplished when constrained by available observations, especially when the  
115 mean state influences transient response as may be the case for sea ice.

116

117 Even if the sea ice mean state can be observationally constrained, internally generated  
118 climate variability obscures the influence of the mean state on the transient sea ice response.  
119 Having many realizations that show the same response increases confidence that a signal results  
120 from a sea ice thickness difference and not from internally generated climate variability. As a  
121 result, large initial-condition ensembles are needed to quantify the influence of mean sea ice state  
122 on sea ice projections. While such ensembles are becoming more standard practice and more  
123 broadly available with CMIP-class models (e.g., Deser et al. 2020), sensitivity tests using large  
124 ensembles as a control are rare. In particular, a targeted experiment that isolates the influence of  
125 sea ice mean state on climate change and variability in a CMIP-class model with a large ensemble  
126 has not been done.

127

128 In this study, we build on previous work by isolating the influence of the sea ice mean state  
129 on climate. We focus on two research questions:

- 130 1) Does sea ice mean state influence the rate and timing of transient anthropogenically  
131 forced sea ice change? In particular, does thicker Arctic sea ice lead to slower sea ice  
132 loss and a later transition to seasonally ice-free conditions in transient projections for  
133 the 21<sup>st</sup> century?
- 134 2) What is the impact of sea ice mean state on key global climate variables (surface  
135 temperature, precipitation, and sea level pressure)? Specifically, can we detect the  
136 influence of sea ice mean state on pre-industrial climate and 1850-2100 transient  
137 climate change and variability in both polar and non-polar regions?

138 To answer our research questions, we modify the sea ice model within an earth system  
139 model to increase surface albedo, reduce surface melt, and increase the mean state sea ice. We  
140 then quantify the influence of the sea ice mean state differences on mean and transient climate  
141 change using a large initial condition ensemble as a control. Working within this numerical  
142 simulation framework, we can isolate differences in transient projections that arise from sea ice  
143 mean state alone. While we present results from both poles, we focus more on the Arctic where  
144 the parameter changes have a larger impact and reduce a model bias. We find that with thicker  
145 sea ice, the transition to an ice-free Arctic Ocean is delayed. In addition, the impacts of sea ice  
146 tuning on non-polar climate are small. While our results rely on one model, our analysis provides  
147 guidance for future modeling development efforts, especially those that hope to optimize their  
148 simulation of transient Arctic sea ice loss.

149

## 150 **2. Methods**

### 151 **2.1 Model simulations and comparison strategies**

152 We use a well-documented state-of-the-art global climate model: the Community Earth  
153 System Model version 2 (CESM2) with the Community Atmosphere Model version 6 (CAM6)  
154 (Danabasoglu et al. 2020). CESM2-CAM6, hereafter shortened to simply CESM2, is an attractive  
155 model to use for two reasons. First, comprehensive simulations exist for CESM2 as a part of the  
156 Coupled Model Intercomparison Project version 6 (CMIP6) (Eyring et al. 2016) and a recently  
157 released large initial-condition ensemble, hereafter referred to as the CESM2-LE (Rodgers et al.  
158 2021). Second, CESM2 has a mean state Arctic sea ice bias. When compared to present-day  
159 observations, CESM2 has insufficient late summer Arctic sea ice cover, a bias that has been  
160 attributed to the sea ice being too thin (Danabasoglu et al. 2020 Figure 17g, DuVivier et al. 2020).  
161 The consequences of this CESM2 thin Arctic sea ice bias for transient sea ice change have been  
162 documented in DeRepentigny et al. (2020). For example, the 11 CESM2 CMIP6 transient  
163 historical simulations have ice-free late summer conditions in the Arctic as early as 2010, which  
164 is inconsistent with satellite observations even when accounting for internal variability.

165

166 Inspired to remedy the CESM2 thin Arctic sea ice bias and assess its impact on the global  
167 climate system, we created CESM2-lessmelt. CESM2-lessmelt is identical to CESM2 except for  
168 two parameter modifications made within the thermodynamics of the sea ice model. The sea ice  
169 model in CESM2 (CICE 5.1.2; Hunke et al. 2015) uses a multiple-scattering Delta-Eddington  
170 radiative transfer parameterization which relies on the specification of inherent optical properties  
171 (Briegleb and Light 2007). These optical properties can be adjusted to change the albedo of snow-

172 covered sea ice. In CESM2-lessmelt, we increased the albedo of snow on sea ice by increasing  
173 the  $r_{\text{snw}}$  parameter from 1.25 to 1.5 standard deviations. This  $r_{\text{snw}}$  parameter change  
174 decreases the dry snow grain radius from 187.5  $\mu\text{m}$  to 125  $\mu\text{m}$ . In addition, we changed the  $dt_{\text{melt}}$   
175 parameter such that the melt onset temperature increases by 0.5  $^{\circ}\text{C}$  from -1.5  $^{\circ}\text{C}$  to -1.0  $^{\circ}\text{C}$ . This  
176 melt onset temperature determines when the snow grain radius starts to grow from a dry snow  
177 value to a melting snow value. Both CESM2-lessmelt parameter changes were implemented to  
178 increase snow albedo, reduce sea ice melt, and increase the mean state sea ice thickness. Both  
179 parameter changes were made globally and thus affect sea ice in both hemispheres. Finally, both  
180 parameter changes are within the observational uncertainty provided by in situ observations from  
181 Surface Heat Budget of the Arctic Ocean (SHEBA).

182

183 In this work, we compare simulations with constant pre-industrial control climate  
184 conditions. For CESM2, we use the multi-century CMIP6 1850 pre-industrial control run. For  
185 CESM2-lessmelt, we ran a 550-year-long CESM2-lessmelt 1850 pre-industrial control run. The  
186 CESM2-lessmelt control was branched from year 881 of the CESM2 CMIP6 control. As a sanity  
187 check, we assessed global metrics of energy conservation and climate stability in the CESM2-  
188 lessmelt control and compared it to the CESM2 control during overlapping years. The global mean  
189 surface temperature is 0.16 K lower in CESM2-lessmelt (288.18 K) than in CESM2 (288.34 K).  
190 The top-of-model energy imbalance in both models is small:  $-0.02 \text{ Wm}^{-2}$  for CESM2-lessmelt and  
191  $0.07 \text{ Wm}^{-2}$  for CESM2. Correspondingly, ocean temperature drift is smaller in CESM2-lessmelt  
192 than in CESM2. Overall, both models exhibit small drift in their global mean surface temperature  
193 and top-of-model energy imbalance. Thus, both CESM2 model versions meet basic energy  
194 conservation and stability criteria for global coupled modeling science.

195

196 In addition to pre-industrial control comparisons, we also compare simulations of 1850-  
197 2100 transient climate change under the same CMIP6 forcing. For CESM2, we use the first 50  
198 ensemble members of the CESM2-LE. As described in Rodgers et al. (2021), members 1-50  
199 share the same transient CMIP6 forcing: historical (1850-2014) and the SSP3-7.0 future scenario  
200 (2015-2100) (O'Neill et al. 2016). For CESM2-lessmelt, we ran a 4-member mini ensemble using  
201 the same historical and SSP3-7.0 CMIP6 forcing as CESM2-LE members 1-50. The first CESM2-  
202 lessmelt ensemble member started at year 1181 of the CESM2-lessmelt 1850 pre-industrial  
203 control run and was run from 1850 to 2100. Three additional CESM2-lessmelt ensemble members  
204 were run from 1920 to 2100 with initial conditions from the first CESM2-lessmelt ensemble  
205 member perturbed by round-off ( $10^{-14}$  K) differences in air temperature.

206 As all transient ensemble members analyzed in this work share the same forcing, we  
207 assume each ensemble member is an equally likely estimate of the transient climate response.  
208 This “equally likely” assumption is justified in the Supporting Information (Text S1, Figures S1-  
209 S5). This assumption enables us to statistically quantify differences between CESM2-LE and  
210 CESM2-lessmelt. Given the differences in ensemble size, we use bootstrapping to statistically  
211 assess when the 4 CESM2-lessmelt ensemble members are distinct from the first 50 members  
212 of the CESM2-LE. Bootstrapping, or randomly resampling to generate statistics, requires no  
213 distribution assumptions.

214  
215 Finally, it is important to note a feature of all transient model simulations analyzed here.  
216 Namely, the CMIP6 historical forcing includes a stark increase in the inter-annual variability of  
217 biomass burning emissions during the satellite era of wildfire monitoring 1997-2014 (Fasullo et al.  
218 2021, DeRepentigny et al. 2021). This discontinuity leads to excessive surface warming in the  
219 northern hemisphere extratropics (Fasullo et al. 2021). It also contributes to 1997-2010 Arctic sea  
220 ice loss followed by a 2010-2025 Arctic sea ice recovery (DeRepentigny et al. 2021). While  
221 several CMIP6 models show impacts from this discontinuity, the CESM2 has a particularly  
222 pronounced response. In this work, we use this discontinuity as an opportunity to assess the  
223 influence of sea ice mean state on the sea ice response to a short-term radiative forcing.

224

### 225 **3. Results**

#### 226 **3.1. Pre-industrial sea ice in CESM2 and CESM2-lessmelt**

227 Comparison of pre-industrial sea ice volume and cover monthly mean values show  
228 CESM2-lessmelt has more sea ice than CESM2 in both hemispheres (Figure 1). In the Arctic, sea  
229 ice volume in CESM2-lessmelt exceeds that in CESM2 during all months (Figure 1a). In contrast,  
230 Arctic sea ice cover differences have a distinct seasonal cycle with large late summer differences  
231 and small winter differences (Figure 1b). In the Antarctic, CESM2-lessmelt has larger sea ice  
232 cover and volume than CESM2 in all months (Figure 1c,d). Monthly mean volume differences  
233 between CESM2 and CESM2-lessmelt are larger in the Arctic (30% greater in CESM2-lessmelt)  
234 than in the Antarctic (8% greater in CESM2-lessmelt). Larger sea ice changes in the Arctic than  
235 in the Antarctic are unsurprising because CESM2 and CESM2-lessmelt differ in their surface melt.  
236 Unlike in the Arctic, surface melt in the Antarctic is negligible. Almost all Antarctic sea ice melts  
237 from below.

238

239           Spatially, the largest sea ice cover differences occur at the summer sea ice edge  
240 where/when the sea ice can expand/contract without influence of land barriers and ocean  
241 circulation. At the late summer seasonal minimum, the CESM2-lessmelt sea ice edge expands  
242 equatorward at the sea ice margin in both hemispheres (Figure 2). Yet, this late summer  
243 expansion in CESM2-lessmelt is not zonally uniform. In the Arctic, the largest late summer ice  
244 concentration increases in CESM2-lessmelt occur north of Russia in the East Siberian Sea  
245 (Figure 2b). In contrast, only modest late summer sea ice expansion happens in the North Atlantic.  
246 In the Antarctic, the largest magnitude late summer sea ice concentration expansion equatorward  
247 occurs off the coast east of the Weddell Sea (Figure 2d). Changes in late-summer Antarctic sea  
248 ice concentration are otherwise small, likely due to the lack of sea ice at the seasonal minimum.  
249 At the seasonal maximum in late winter, Arctic concentrations differences are small due to the  
250 land barriers and the ocean heat convergence that controls the sea ice edge (Figure 3a-b; Bitz et  
251 al. 2005). In the Antarctic, the late winter sea ice edge has a zonally non-uniform response with  
252 some regions exhibiting sea ice concentration increases and others exhibiting sea ice  
253 concentration decreases (Figure 3c-d). In particular, there is slightly less sea ice cover in CESM2-  
254 lessmelt than in CESM2 in the Ross Sea. Non-zonally asymmetric sea ice differences  
255 demonstrate the importance of both thermodynamic and dynamic responses to the sea ice  
256 parameter changes made in CESM2-lessmelt.

257  
258           Sea ice thickness comparisons are also of interest, especially in the Arctic where thicker  
259 late winter sea ice can lead to less late summer sea ice loss. Unlike the concentration differences  
260 that manifested at the sea ice edge, sea ice thickness differences at the late winter seasonal  
261 maximum occur throughout the sea ice pack (Figure 4). Late-winter sea ice thicknesses are at  
262 least 0.5 m greater in CESM2-lessmelt than in CESM2 throughout the central Arctic basin (Figure  
263 4b). Antarctic sea ice thickness differences are much smaller, generally less than 0.25 meters  
264 (Figure 4d). The largest differences in the Antarctic occur off the west side of the Antarctic  
265 Peninsula in the Bellingshausen Sea.

266  
267           To quantify processes underlying the mean state differences between the two CESM2  
268 model variants, we next compare their sea ice mass tendencies. In addition to analyzing the total  
269 sea ice mass tendency, we also decompose this total tendency into contributions from dynamic  
270 and thermodynamic processes. Dynamic mass tendencies result from advection of ice into or out  
271 of a grid cell. Thermodynamic mass tendencies result from the sum of basal ice growth, ice growth  
272 in supercooled open water, transformation of snow to sea ice, surface melting, lateral melting,

273 basal melting and evaporation/sublimation. See DuVivier et al. (2020), Singh et al (2021), and  
274 Bailey (2020) for more information about these diagnostics including their application to evaluate  
275 CESM2 sea ice. Consistent with a balanced mean state and negligible model drift, the annual  
276 mean tendency terms differences are small (not shown). Yet, substantial differences in the sea  
277 ice mass tendency terms occur during both the growth season and the melt season in both  
278 hemispheres in response to the parameter changes made in CESM2-lessmelt.

279  
280 Arctic sea ice mass tendency diagnostics show CESM2 and CESM2-lessmelt differences  
281 result from both thermodynamics and dynamics (Figure 5). During the melt season, CESM2-  
282 lessmelt has less Arctic thermodynamic sea ice mass loss than CESM2. This thermodynamic sea  
283 ice mass loss difference is consistent with a higher snow albedo in CESM2-lessmelt than in  
284 CESM2. CESM2-lessmelt also has less thermodynamic Arctic sea ice mass gain than CESM2  
285 during the growth season due to the negative ice-thickness growth feedback (Bitz and Roe, 2004).  
286 These opposing seasonal influences on thermodynamic tendency terms are consistent with  
287 thicker Arctic sea ice in CESM2-lessmelt than in CESM2. Dynamical sea ice tendency terms  
288 dominate at the sea ice edge and during the growth season, and result primarily from the same  
289 ice velocity transporting thicker ice. With its thicker sea ice, CESM2-lessmelt has more ice export  
290 out of and more ice transport within the Arctic basin than CESM2. When more ice is moved into  
291 a region where sea ice can melt, thermodynamic mass tendencies and dynamic mass tendencies  
292 compensate.

293  
294 We next evaluate sea ice mass tendencies for CESM2 and CESM2-lessmelt in the  
295 Antarctic (Figure 6). Positive dynamic mass tendencies increase sea ice away from the Antarctic  
296 coast in all seasons. This dynamically driven sea ice mass increases result from wind-driven  
297 transport of sea ice away from the Antarctic coast. During the growth season, thermodynamically-  
298 driven sea ice mass gains occur near the coast, which in turn increases dynamically-driven sea  
299 ice mass gains away from the coast. When compared to CESM2, CESM2-lessmelt has more  
300 dynamical mass gain associated with this wind-driven sea ice advection in all seasons. As in the  
301 Arctic, these CESM2 – CESM-lessmelt differences result primarily from sea ice thickness  
302 changes with a similar sea ice velocity field. During the melt season, sea ice mass loss due to  
303 thermodynamics is less in CESM2-lessmelt than in CESM2. Yet, the growth season in the  
304 Antarctic differs from that in the Arctic. Unlike in the Arctic, the Antarctic has little multi-year ice  
305 and thus minimal ice-thickness growth feedback. Also unlike the Arctic, the Antarctic gains mass  
306 through snow-ice formation.

307 **3.2. Influence of sea ice tuning on pre-industrial global climate**

308 Overall, CESM2-lessmelt and CESM2 have statistically significant differences in surface  
309 air temperature, precipitation, and sea level pressure at both poles (Figure 7). In contrast, impacts  
310 on non-polar climate are small and not statistically significant. Where CESM2-lessmelt has more  
311 sea ice than CESM2, the Arctic and Antarctic surface are both cooler in CESM2-lessmelt than in  
312 CESM2, especially in non-summer seasons. Demonstrating the importance of sea ice to polar  
313 surface temperatures, Ross Sea air temperatures increased in CESM2-lessmelt when compared  
314 to CESM2, consistent with sea ice concentration and thickness decreases from CESM2-lessmelt  
315 to CESM2 in this region (Figure 3d, Figure 4d). Generally speaking, precipitation differences  
316 between CESM2 and CESM2-lessmelt followed surface temperature differences. The relatively  
317 cooler CESM2-lessmelt atmosphere converges less moisture and has less precipitation,  
318 especially in Fall in the Arctic. Despite this precipitation reduction, CESM2-lessmelt has 10% more  
319 snow on Arctic sea ice in spring than CESM2, which is in better agreement with observations  
320 (Webster et al., 2021). More snow on sea ice in CESM2-lessmelt than in CESM2 results from a  
321 CESM2-lessmelt having a larger sea ice platform to collect snow than CESM2, especially during  
322 the peak snowfall season (Fall). Overall, polar sea level pressure differences are generally small  
323 and not statistically significant. One notable exception are statistically significant sea level  
324 pressure differences between CESM2 and CESM2-lessmelt during Arctic Fall, including the well-  
325 known atmospheric circulation response to boundary layer thermal forcing (e.g., Deser et al.  
326 2010). Here, boundary layer cooling in CESM2-lessmelt leads to a local high SLP response in  
327 autumn (baroclinic vertical structure).

328

329 In addition to mean climate state, we also assessed climate variability differences arising  
330 from the different sea ice mean states in CESM2 and CESM2-lessmelt. In brief, climate variability  
331 differences between the multi-century CESM2 and CESM2-lessmelt pre-industrial control runs  
332 are small and not statistically significant. Major modes of climate variability, such as those plotted  
333 in the Climate Variability Diagnostics Package (Phillips et al 2020), are unchanged between  
334 CESM2 and CESM2-lessmelt pre-industrial control runs. Similarly, differences in inter-annual  
335 seasonal surface temperature, sea level pressure, and precipitation standard deviations are small  
336 and not statistically significant (Figure S6).

337

338 **3.3. Transient (1850-2100) sea ice evolution in CESM2 and CESM2-lessmelt**

339 Present-day (1979-2014) monthly hemispheric mean differences (Figure 8) resemble  
340 corresponding pre-industrial control differences (Figure 1). In the Arctic, CESM2-lessmelt has

341 more present-day sea ice volume than CESM2 in every month (Figure 8a). Moreover, CESM2-  
342 lessmelt also has more present-day Arctic sea ice cover than CESM2 in all months, with the  
343 largest differences during the melt season and especially in late summer (Figure 8b-c). Overall,  
344 the Arctic sea ice mean state is closer to observations in CESM2-lessmelt than in CESM2. Of  
345 particular note, additional present-day late summer Arctic sea ice cover brings CESM2-lessmelt  
346 closer to observations than CESM2. While present-day hemispheric multi-decadal Arctic sea ice  
347 volume observations are not available (Massonnet et al. 2018), reductions in late-summer sea ice  
348 cover biases may suggest CESM2-lessmelt has a more realistic sea ice volume than CESM2.  
349 Like in the Arctic, present-day Antarctic sea ice differences between CESM2 and CESM2-  
350 lessmelt are also qualitatively similar to the pre-industrial control (Figure S7). But unlike in the  
351 Arctic, both CESM2 variants have substantial Antarctic mean state biases without consistent bias  
352 reduction from CESM2 to CESM2-lessmelt. Given similar Antarctic sea ice biases, relatively  
353 modest Antarctic mean state sea ice changes, and the inability of CESM2 and CESM2-lessmelt  
354 to reproduce observed Antarctic sea trends (Figure S8), we focus on the Arctic for the remainder  
355 of the transient sea ice comparisons.

356  
357 Arctic maps reveal that the sea ice in CESM2 and CESM2-lessmelt evolves differently  
358 from the present-day into the 21<sup>st</sup> century (Figure 9). While both CESM2 and CESM2-lessmelt  
359 have their greatest present-day (1979-2014) late winter sea ice thicknesses and late summer sea  
360 ice concentrations north of Greenland and the Canadian Archipelago, CESM2-lessmelt has more  
361 sea ice throughout much of the Arctic Ocean than CESM2 (Figure 9a-d). Notably, September  
362 Arctic sea ice concentrations are substantially greater in CESM2-lessmelt than in CESM2 (Figure  
363 9c). Equally important, the present-day March sea ice is 0.5+ meters thicker in CESM2-lessmelt  
364 than in CESM2 over most of the central Arctic Ocean (Figure 9d). By 2030-2049, Arctic sea ice  
365 differences between CESM2-lessmelt and CESM2 remain for late-summer September  
366 concentration but are small for late winter March thickness (Figure 9e-f). Large 2030-2049 late  
367 summer ice cover differences occur because despite starting the melt season with similar March  
368 sea ice thickness distributions, less melt occurs in CESM2-lessmelt than in CESM2. This  
369 difference in 2030-2049 summer melt is consistent with higher albedo in CESM2-lessmelt than in  
370 CESM2. By 2050-2069, CESM2 and CESM2-lessmelt have similar small September sea ice  
371 concentrations (Figure 9g). Consistent with a transition to a seasonally ice-free Arctic, March sea  
372 ice thicknesses are also similar in 2050-2069 over much of the Arctic Ocean (Figure 9h). In fact,  
373 the only regions where 2050-2069 differences between CESM2-lessmelt and CESM2 persist are

374 along the coast of Northern Greenland and the far North Eastern portions of the Canadian  
375 archipelago.

376

377 While ensemble means provide the most robust assessment of the differences in CESM2  
378 and CESM2-lessmelt, ensemble mean values are not physically realized quantities, mute internal  
379 variability, and thus should not be compared as equals with observed timeseries and trends.  
380 Instead, each individual CESM2-LE or CESM2-lessmelt ensemble member's time evolution  
381 should be treated as equally likely and the observations should be treated as the single real world  
382 ensemble member. Consistent with time-averaged ensemble mean comparisons (Figure 8),  
383 September Arctic sea ice extent in all four CESM2-lessmelt ensemble members (Figure 10b) is a  
384 better match to 1979-2020 observations than any of the 50 CESM2-LE ensemble members  
385 (Figure 10a). Up until ice-free conditions are reached, CESM2-lessmelt ensemble members have  
386 more September sea ice extent than almost all of the CESM2-LE ensemble members. Unlike sea  
387 ice amount, 20-year linear trends in September Arctic sea ice in CESM2-LE, CESM2-lessmelt,  
388 and observations largely overlap (Figure 10c). In other words, CESM2-lessmelt and CESM2-LE  
389 trends are both consistent with observed trends. Due to ensemble size differences, the spread in  
390 CESM2-lessmelt trends is smaller than the spread in CESM2-LE trends. Thus, even though  
391 CESM2-lessmelt trends are more negative than observed trends with end dates of 2001-2006,  
392 this may simply be the consequence of ensemble size differences. As introduced in section 2.1  
393 and in DeRepentigny et al. (2021), the individual ensemble members show sea ice loss  
394 accelerates around the turn of the 21<sup>st</sup> century and then the sea ice recovers in the early 21<sup>st</sup>  
395 century due to the prescribed biomass burning emissions in CMIP6 forcing.

396

397 Continuing with the equally likely framework in mind, we next assess common metrics  
398 used for sea ice model evaluation: sea ice sensitivity and the timing of a seasonally ice-free Arctic  
399 (Figure 11). These metrics illustrate the challenge of large internally driven variability for  
400 differentiating between CESM2-lessmelt and CESM2-LE and comparing them to our single  
401 observed reality. For September 1979-2014 Arctic sea ice extent trends, there is substantial  
402 spread across the CESM2-LE members (Figure 11a). Despite this large CESM2-LE spread, the  
403 observations and the CESM2-lessmelt ensemble members are on the smaller trend side of the  
404 distribution. Notably, the observations and one CESM2-lessmelt ensemble member are outside  
405 of the CESM2-LE spread. Similarly, the sea ice sensitivity per global mean warming appears  
406 larger in CESM2-lessmelt with three out of four ensemble members outside of the spread of the  
407 CESM2-LE (Figure 11b). Given the single observed reality and the 4 CESM2-lessmelt members,

408 the spread in CESM2-LE sea ice trends and global mean warming is large and humbling.  
409 Assuming any individual ensemble member is equally likely, the large spread in these metrics  
410 provide limited value as a model comparison metric for evaluating CESM2-LE and CESM2-  
411 lessmelt because the CESM2-lessmelt ensemble is so small (4 members).

412  
413 Internal variability also has a strong imprint on the timing of a first seasonally ice-free Arctic  
414 Ocean. Indeed, the CESM2-LE exhibits a 38 year spread in this metric with years ranging from  
415 2007 to 2045 (Figure 11c). While the spread in the CESM2-lessmelt first ice-free Arctic year is  
416 small (2041 to 2057), the 4 CESM2-lessmelt first ice-free years barely overlap with the 50 CESM2-  
417 LE first ice-free years. Bootstrapping the CESM2-LE ice-free dates shows the two distributions  
418 are statistically different at the 95% confidence level. In other words, the thicker and more  
419 extensive Arctic sea ice in CESM2-lessmelt delays the timing of an ice free Arctic when compared  
420 to CESM2-LE. While the delay of the first ice-free Arctic is statistically significant, the large  
421 internally generated variability still limits its predictability by decades. The spread in ice-free years  
422 in the first 50 members of the CESM2-LE is made especially large and early by the accelerated  
423 sea ice decline associated with the CMIP6 biomass burning emissions (DeRepentigny et al.  
424 2021).

425  
426 We next use ensemble means to quantify forced response differences between CESM-  
427 LE and CESM2-lessmelt (Figure 12). To make consistent forced response comparisons, we  
428 bootstrap the 50 CESM2-LE members to generate statistics that are consistent with ensembles  
429 with only four members. With these bootstrapped values, we can statistically assess when  
430 CESM2-lessmelt and CESM2-LE differ while accounting for differences in ensemble size. For  
431 example, if the CESM2-lessmelt ensemble mean lies outside of the 95% confidence limits of  
432 sample statistics generated randomly by selecting 4 members of the CESM2-LE many times (here  
433 1,000 times), the forced response differences are statistically significant. Comparing the  
434 ensemble means consistent with four ensemble members, we find that CESM2-lessmelt has more  
435 September sea ice extent (Figure 12a) and more March sea ice volume (Figure 12b).  
436 Interestingly, twenty-year trends in September sea ice extent and March sea ice volume are  
437 statistically indistinguishable in CESM2-lessmelt and CESM2-LE with the exception of three  
438 periods (Figure 12c-d). The first exception is for the period with trend end dates ~2010 during the  
439 biomass burning forcing discontinuity. During this time period, the CESM2-lessmelt has less  
440 negative sea ice extent trends and more negative sea ice volume trends than the CESM2-LE.  
441 This first exception is consistent with the thicker sea ice in CESM2-lessmelt being more resilient

442 to ice cover changes but more sensitive to ice volume changes due to a weaker thickness-ice  
443 growth feedback. The second time period when there are trend differences occurs in the 2060s  
444 and 2070s. This exception occurs because CESM2-lessmelt still has ice to lose while CESM2-LE  
445 is ice-free already in September (Figure 11). As a result, CESM2-lessmelt has more negative  
446 September sea ice extent trends than CESM2-LE during the 2060s and 2070s. Similar trend  
447 differences associated with timing differences to an ice-free Arctic are seen in October and  
448 August, but shifted later in the 21<sup>st</sup> century (not shown). The last time period is for trend end dates  
449 around 1970 when the volume trends in CESM2-lessmelt are larger than those in CESM2-LE.

450

451 We finish comparing the 1850-2100 transient sea ice evolution by contrasting interannual  
452 sea ice variability in CESM2-lessmelt and CESM2-LE. As was done for means, we bootstrap the  
453 CESM2-LE to create variability estimates consistent with an ensemble with only 4 members.  
454 Consistent with previous work (Goosse et al. 2009, Mioduszewski et al. 2019), we find Arctic sea  
455 ice cover variability strongly depends on the mean sea ice thickness in CESM2-LE and CESM2-  
456 lessmelt (Figure S9). Overall, September sea ice extent interannual variability is smaller in  
457 CESM2-lessmelt than in CESM2-LE until the middle of the 21<sup>st</sup> century. Smaller September sea  
458 ice variability in CESM2-lessmelt is especially seen during the turn of the century forced sea ice  
459 decline (20 year trends ending ~2010). After the 2040s, CESM2-lessmelt has more year-to-year  
460 September sea ice extent variability than CESM2-LE because CESM2-lessmelt transitions to a  
461 seasonally ice-free Arctic later than CESM2-LE.

462

### 463 **3.4. Influence of sea ice mean state on transient climate change**

464 We next assess the impact of the differing CESM2-LE and CESM2-lessmelt 1850-2100  
465 sea ice evolution on transient climate change more broadly. In the end, we focus on surface  
466 warming for two reasons. First, climate impacts often scale with surface warming. As a result,  
467 assessing where/when warming differences occur provides a foundation for assessing if the  
468 CESM2-LE and CESM2-lessmelt sea ice evolution differences impact climate change and  
469 variability more broadly. Second, we investigated other climate variables such as precipitation  
470 and sea level pressure and found that differences in the transient climate response in CESM-LE  
471 and CESM2-lessmelt were small and not statistically significant (e.g., Figure S10). One exception  
472 was smaller 21<sup>st</sup> century winter Arctic precipitation increases in CESM2-lessmelt than in CESM2-  
473 LE. This exception is consistent with Clausius–Clapeyron relation, namely a reduced water vapor  
474 increase associated with less warming in CESM2-lessmelt than in CESM2-LE.

475

476           When plotted as anomalies, the 1850-2100 evolution of the global mean surface  
477 temperature anomaly in CESM2-LE and CESM2-lessmelt are indistinguishable (Figure 13a). Both  
478 CESM2 model variants are consistent with the observed global air surface temperature anomaly  
479 evolution (Hansen et al. 2010, Rohde and Hausfather 2020). When plotted as absolute values,  
480 the global mean surface temperature is lower in CESM2-lessmelt than CESM2-LE (Figure 13b).  
481 This absolute temperature difference between the two CESM2 variants remains constant over the  
482 entire 1850-2100 period. Given the challenges of observing the absolute global mean temperature  
483 and the spread due to internal variability, it is unclear if CESM2-LE or CESM2-lessmelt provides  
484 a more realistic representation of global mean temperature. Moreover, the spatial pattern of  
485 seasonal warming in CESM2-lessmelt and CESM2 is statistically indistinguishable aside from two  
486 notable and sizable exceptions in the Arctic (Figure 14). First, CESM2-lessmelt warms more than  
487 CESM2-LE along the sea ice edge during Fall, particularly in the Pacific sector. This larger  
488 warming occurs because CESM2-lessmelt has more sea ice to lose in these regions than  
489 CESM2-LE (Figure 2b). Second, CESM2-LE warms more than CESM2-lessmelt in the central  
490 Arctic Ocean during winter. This difference arises because CESM2-LE has thinner sea ice than  
491 CESM2-lessmelt. Finally, the Atlantic Meridional Overturning Circulation (AMOC) weakens  
492 slightly (<10%) more in the CESM2-lessmelt members than in the CESM2-LE leading to small  
493 differences in the North Atlantic warming hole.

494  
495           While the total zonal mean warming over the period 1920-1939 to 2080-2099 is  
496 remarkably similar in CESM2 and CESM2-lessmelt, when that warming happens differs between  
497 the two model variants in the Arctic. Indeed, comparisons of zonal mean warming rates in CESM2  
498 and CESM2-lessmelt show differences in the Arctic warming rates in all seasons except summer  
499 (Figure 15). In particular, CESM2-LE has large non-summer surface Arctic warming rates earlier  
500 than CESM2-lessmelt. These larger early warming rates in CESM2-LE results from an earlier  
501 transition towards an ice-free Arctic Ocean in CESM2-LE than in CESM2-lessmelt.

502

#### 503 **4. Summary and Discussion**

504           This study assesses the influence of sea ice mean state on simulated climate change and  
505 variability in a state-of-the-art global coupled climate model. Novel and new here, a large 50-  
506 member large ensemble is leveraged as a control for assessing the new small 4-member  
507 ensemble with more mean state sea ice, especially in the Arctic. As large initial condition  
508 ensembles are generally run after model releases, we address a question that is unanswerable  
509 during model development: Do differences in the sea ice mean state alter the ensemble spread

510 of realized transient climate change? Our results re-enforce that a realistic Arctic mean state is  
511 critical to simulating a realistic transition to an ice-free Arctic Ocean. Specifically, simulations with  
512 the same global warming but more Arctic sea ice have a later transition to a late summer ice-free  
513 Arctic over the 21<sup>st</sup> century. These results demonstrate starting with a reasonable mean state is  
514 important for trusting model-projected timing towards an ice-free Arctic Ocean in a warming world.  
515 Important for climate projections and model development more generally, the sea ice differences  
516 examined here had negligible impacts outside the polar regions. It is important to emphasize that  
517 the magnitude of the sea ice influence on polar and non-polar climate is similar to recent inter-  
518 model comparison studies (e.g., Screen et al. 2018, Smith et al. 2021). Yet, the context here is  
519 different. Specifically, the differences between CESM2 and CESM2-lessmelt outside of the Arctic  
520 are small in the context of model development/climate impacts, especially for transient climate  
521 change with multiple ensemble members. The model configuration presented here (CESM2-  
522 lessmelt) is a viable model for coupled model experimentation. We anticipate and advise the use  
523 of CESM2-lessmelt for prediction and hypothesis-driven experiments focused on the Arctic.

524

525         Interestingly, many commonly used metrics to benchmark sea ice simulations provide  
526 limited value in this study. Assuming any individual ensemble member is equally likely, many  
527 metrics struggle to differentiate between the thicker (CESM2-lessmelt) and thinner (CESM2) sea  
528 ice model variants examined here. For example, this study reinforces previous work showing a  
529 two decade uncertainty in the timing of an ice-free Arctic due to internally generated variability  
530 (Jahn et al. 2016, Notz 2015). Here, we find an almost four decade uncertainty in the timing of an  
531 ice-free Arctic in the first 50 members of the CESM2-LE due to the confluence of CMIP6 biomass  
532 burning forcing and thin CESM2 Arctic sea ice. In addition, sea ice sensitivity (i.e., sea ice change  
533 scaled by global warming) exhibits large spread in the first 50 CESM2-LE members and thus  
534 provides limited value as an observational constraint or a robust model comparison metric to  
535 CESM2-lessmelt. Finally, linear 20-year sea ice area trends were similar between CESM2 and  
536 CESM2-lessmelt ensemble members. That said, CESM2-lessmelt is consistent the observed  
537 trend while CESM2-LE is not when trends longer than 20 years are considered (e.g., 1979-2014  
538 following Notz, D. and the SIMIP Community (2020)). The fact that many commonly used metrics  
539 provide limited differentiation in this study is sobering and merits emphasis. Internal variability is  
540 large and must be measured and accounted for when comparing model ensemble size, as was  
541 done here. Of course, these findings are not entirely surprising given similar global warming in  
542 CESM2 and CESM2-lessmelt. In other words, global warming cannot be used as constraint on  
543 simulated sea ice trends or sensitivity in this study. In fact, the mean state differences probed

544 here were not large enough to cause Arctic sea ice trend differences for the same amount of  
545 global warming. As a result, this work does not refute previous work showing that global warming  
546 (e.g., Mahlstein and Knutti 2012, Roach et al. 2020, Notz, D. & SIMIP Community 2020, Horvat  
547 2021) can constrain sea ice change, and can help illustrate when models have the right Arctic  
548 sea ice trends for the wrong reasons (e.g., Rosenblum and Eisenman 2017). In summary, the  
549 similarity between CESM2 and CESM2-lessmelt found here provides further evidence that global  
550 warming exerts strong controls on Arctic sea ice trends.

551

552 We end by discussing lessons learned for simulation of sea ice in a global coupled climate  
553 modeling framework. We began this study by reducing sea ice surface melt in a pre-industrial  
554 control simulation in search of a stable model configuration with more Arctic Ocean sea ice volume  
555 and late summer Arctic Ocean sea ice cover. The parameter modifications implemented in  
556 CESM2-lessmelt were specifically targeted to reduce summer melt in the Arctic where surface  
557 melt dominates. Unlike the Arctic, Antarctic sea ice melt is dominated by bottom melt. Thus, we  
558 anticipated and found relatively small differences in the Antarctic sea ice mean state as a result  
559 of our parameter modifications. After obtaining a stable multi-century control run, we then ran  
560 transient 1850-2100 simulations with no additional changes. What emerged in the transient  
561 simulations was influenced both by the mean state and by feedbacks in CESM2, and was a  
562 surprise to us. Indeed, our success in obtaining more realistic transition to an ice-free Arctic state  
563 with CESM2-lessmelt suggests that sea ice thickness and late summer cover are important  
564 targets for sea ice in coupled model development. In contrast, attention to and tuning of Arctic  
565 sea ice area alone is generally insufficient. That said, sea ice area expansion is important to  
566 monitor and model development should focus on parameters and physics that lead to credible  
567 sea ice area distributions. The North Atlantic is especially important to monitor as when sea ice  
568 expands to completely cover the ocean there, it can shut down North Atlantic deep water  
569 formation, and derail global coupled earth system model development as discussed in  
570 Danabasoglu et al. (2020).

571

572

573

574

575

576

577 **Acknowledgments and Data**

578  
579  
580  
581  
582  
583  
584  
585  
586  
587  
588  
589  
590  
591  
592  
593  
594  
595  
596  
597  
598  
599  
600  
601  
602

J.E.K. was supported by National Science Foundation (NSF) CAREER 1554659. P. D. was supported by the Natural Sciences and Engineering Council of Canada (NSERC), the Fond de recherche du Québec – Nature et Technologies (FRQNT) and the Canadian Meteorological and Oceanographic Society (CMOS) through Ph.D. scholarships and by NSF CAREER 1554659, and NSF CAREER 1847398. M.M.H., D.A.B., A.D., C.D., J.E., and N.R. acknowledge support by the National Center for Atmospheric Research (NCAR), which is a major facility sponsored by the NSF under Cooperative Agreement 1852977. M. M. H. was additionally supported by NSF-OPP 1724748. A.J. was supported by NSF CAREER 1847398. M.M.S. was supported by NSF OPP-1724467 and OPP-172474. M.A.W. was provided by NASA's New (Early Career) Investigator Program in Earth Science Award 80NSSC20K0658. S.-S.L. and K.B.R. were supported by IBS-R028-D1. The CESM project and NCAR are supported primarily by NSF. All authors thank the two anonymous reviewers for their constructive and helpful reviews. Computing and data storage resources for developing CESM2, CESM2-lessmelt, and CESM2-LE were provided by the Computational and Information Systems Laboratory (CISL) at NCAR, including the Cheyenne supercomputer (doi:10.5065/D6RX99HX). The CESM2-LE simulations were run on the IBS/ICCP supercomputer "Aleph", a 1.43 petaflop high-performance Cray XC50-LC Skylake computing system with 18,720 processor cores, with 9.59 petabytes of disc storage, and 43 petabytes of tape archive storage. CESM2-LE data are available here: <https://www.cesm.ucar.edu/projects/community-projects/LENS2/>. The CESM2-lessmelt data are available via Globus access to NCAR GLADE at: [/glade/campaign/cgd/ppc/cesm2\\_tuned\\_albedo](https://glade/campaign/cgd/ppc/cesm2_tuned_albedo). For more information on using Globus on NCAR systems, please refer to <https://www2.cisl.ucar.edu/resources/storage-and-file-systems/globus-file-transfers>

603 **References**

- 604 Bailey, D. A., Holland, M. M., DuVivier, A. K., Hunke, E. C., & Turner, A. K. (2020), Impact of a  
605 new sea ice thermodynamic formulation in the CESM2 sea ice component. *Journal Of*  
606 *Advances In Modeling Earth Systems*, 12, e2020MS002154. doi:10.1029/2020MS002154
- 607 Bitz, C. M, Holland, M. M., Hunke, E. & Moritz, R. E. (2005), Maintenance of the sea-ice edge, *J.*  
608 *Climate*, 18, 2903-2921.
- 609 Bitz, C. M. (2008), Some aspects of uncertainty in predicting sea ice thinning, in Arctic Sea Ice  
610 Decline: observations, projections, mechanisms, and implications, AGU Geophysical  
611 Monograph Series, vol, edited by E. deWeaver, C. M. Bitz, and B. Tremblay, pp. 63-76 ,  
612 American Geophysical Union.
- 613 Bitz, C. M. & Roe, G. H. (2004), A Mechanism for the High Rate of Sea-Ice Thinning in the Arctic  
614 Ocean, *J. Climate*, 17, 3622--31
- 615 Blanchard-Wrigglesworth E., Bitz, C.M. & Holland, M.M. (2011). Influence of initial conditions and  
616 climate forcing on predicting Arctic sea ice, *Geophysical Research Letters*, 38, L18503,  
617 doi: 10.1029/2011GL048807
- 618 Bonan, D. B., Lehner, F. & Holland, M. (2021), Partitioning uncertainty in projections of Arctic sea  
619 ice, *Environmental Research Letters*, DOI: 10.1088/1748-9326/abe0ec
- 620 Briegleb, B. P., & Light, B. (2007), A delta-Eddington multiple scattering parameterization for  
621 solar radiation in the sea ice component of the Community Climate System Model. NCAR  
622 Tech. Note TN-4721STR, 100 pp.
- 623 Danabasoglu, G., Lamarque, J.-F., Bachmeister, J., Bailey, D. A., DuVivier, A. K., Edwards, J.,  
624 Emmons, L. K., Fasullo, J., Garcia, R., Gettelman, A., Hannay, C., Holland, M. M., Large,  
625 W. G., Lawrence, D. M., Lenaerts, J. T. M., Lindsay, K., Lipscomb, W. H., Mills, M. J.,  
626 Neale, R., Oleson, K. W., Otto-Bliesner, B., Phillips, A. S., Sacks, W., Tilmes, S., van  
627 Kampenhout, L., Vertenstein, M., Bertini, A., Dennis, J., Deser, C., Fischer, C., Fox-  
628 Kemper, B., Kay, J. E., Kinnison, D., Kushner, P. J., Long, M. C., Mickelson, S., Moore, J.  
629 K., Nienhouse, E., Polvani, L., Rasch, P. J., & Strand, W. G. (2020), The Community Earth  
630 System Model version 2 (CESM2). *Journal of Advances in Modeling Earth Systems*, 12,  
631 e2019MS001916. <https://doi.org/10.1029/2019MS001916>
- 632 DeRepentigny, P., Jahn., A., Holland, M. M., Fasullo, J., Lamarque, J.-F., Hannay, C., Mills, M.  
633 J., Bailey, D. Tilmes, S., & Barrett, A. (2021), Enhanced early 21st century Arctic sea ice  
634 loss due to CMIP6 biomass burning emissions, *Nature Climate Change*, under review,  
635 Available here: <https://bit.ly/3Ahkjj1>
- 636 DeRepentigny, P., Jahn, A., Holland, M. M., & Smith, A. (2020), Arctic sea ice in the two

637 Community Earth System Model Version 2 (CESM2) configurations during the 20th and  
638 21st centuries. *Journal of Geophysical Research: Oceans*, 125, e2020JC016133.  
639 <https://doi.org/10.1029/2020JC016133>

640 Deser, C., Lehner, F., Rodgers, K.B. et al. (2020), Insights from Earth system model initial-  
641 condition large ensembles and future prospects. *Nat. Clim. Chang.* 10, 277–286,  
642 <https://doi.org/10.1038/s41558-020-0731-2>

643 Deser, C., R. Knutti, S. Solomon, & Phillips, A. S. (2012), Communication of the role of  
644 natural variability in future North American climate. *Nat. Climate Change*, 2, 775–779,  
645 doi:10.1038/nclimate1562.

646 Deser, C., R. Tomas, M. Alexander, & Lawrence, D. (2010), The seasonal atmospheric  
647 response to projected Arctic sea ice loss in the late 21st century. *J. Climate*, 23, 333-351,  
648 10.1175/2009JCLI3053.1.

649 DuVivier, A., Holland, M., Kay, J. E., S. Tilmes, A. Gettelman, & Bailey, D. (2020), Arctic and  
650 Antarctic sea ice state in the Community Earth System Model Version 2, *Journal of*  
651 *Geophysical Research—Oceans*, <http://dx.doi.org/10.1029/2019JC015934>

652 Eyring, V., Bony, S., Meehl, G. A., Senior, C. A., Stevens, B., Stouffer, R. J., & Taylor, K. E.  
653 (2016), Overview of the Coupled Model Intercomparison Project Phase 6 (CMIP6)  
654 experimental design and organization, *Geosci. Model Dev.*, 9, 1937–1958,  
655 <https://doi.org/10.5194/gmd-9-1937-2016>.

656 England, M., Jahn, A., & Polvani, L. (2019), Nonuniform Contribution of Internal Variability to  
657 Recent Arctic Sea Ice Loss, *J. Climate*, DOI: 10.1175/JCLI-D-18-0864.1

658 Fasullo, J. T., Lamarque, J-F, Hannay, C., Rosenbloom, N., Tilmes, S., DeRepentigny, P., Jahn,  
659 A., & Deser, C. (2021). Spurious Late Historical-Era Warming in CESM2 and Other CMIP6  
660 Climate Simulations Driven by Prescribed Biomass Burning Emissions, *Nature Climate*  
661 *Change*, under review, Available here: <https://bit.ly/360yXNv>

662 Fetterer, F., K. Knowles, W. N. Meier, M. Savoie, & Windnagel, A. K. (2017), Sea Ice Index,  
663 Version 3. [1979-2020]. Boulder, Colorado USA. NSIDC: National Snow and Ice Data  
664 Center. doi: <https://doi.org/10.7265/N5K072F8>.

665 Gosse, H., Arzel., O., Bitz, C. M., de Montety, A., & Vancoppenolle, M. (2009) Increased  
666 variability of the Arctic summer ice extent in a warmer climate, *Geophys. Res. Lett.*, 36,  
667 L23702, <https://doi.org/10.1029/2009GL040546>, 2009

668 Hansen, J., Ruedy, R., Sata, M., & Lo, K. (2010), Global surface temperature change, *Rev.*  
669 *Geophys.*, 48, RG4004, doi:10.1029/2010RG000345

670 Holland, M.M., L. Landrum, D. Bailey, & Vavrus, S.J. (2019), Changing seasonal predictability

671 of Arctic summer sea ice area in a warming climate. *J. Climate*, doi:10.1175/JCLI-D-19-  
672 0034.1

673 Holland, M.M., D.A. Bailey, & Vavrus, S. (2011), Inherent sea ice predictability in the rapidly  
674 changing Arctic environment of the Community Climate System Model, version 3, *Climate*  
675 *Dynamics*, 36, 1239-1253, doi:10.1007/s00382-010-0792-4.

676 Holland, M.M., & Stroeve, J. (2011), Changing seasonal sea ice predictor relationships in a  
677 changing Arctic climate. *Geophys. Res. Lett.*, 38, L18501, doi:10.1029/2011GL049303.

678 Holland, M. M., M. C. Serreze, & Stroeve, J. (2010), The sea ice mass budget of the Arctic and  
679 its future change as simulated by coupled climate models, *Climate Dynamics*, 34, 185–  
680 200, doi:10.1007/s00382-008-0493-4.

681 Holland, M.M., C.M. Bitz, & Tremblay, B. (2006), Future abrupt reductions in the Summer Arctic  
682 sea ice, *Geophys. Res. Lett.*, 33, L23503, doi:10.1029/2006GL028024.

683 Horvat, C. (2021), Marginal ice zone fraction benchmarks sea ice and climate model skill, *Nat*  
684 *Communications*, 12, 2221 (2021). <https://doi.org/10.1038/s41467-021-22004-7>

685 Hunke E. C., W. H. Lipscomb, A. K. Turner, N. Jeffery, & Elliott, S. (2015), CICE: The Los Alamos  
686 Sea Ice Model. Documentation and Software User's Manual. Version 5.1. T-3 Fluid  
687 Dynamics Group, Los Alamos National Laboratory, Tech. Rep. LA-CC-06-012.

688 Jahn, A. (2018), Reduced probability of ice-free summers for 1.5 °C compared to 2 °C warming.  
689 *Nature Climate Change*, 8: 409-413. DOI: 10.1038/s41558-018-0127-8

690 Jahn, A., Kay, J. E., Holland, M. M., & Hall, D. M. (2016). How predictable is the timing of a  
691 summer ice-free Arctic?. *Geophysical Research Letters*, 43(17): 9113-9120. DOI:  
692 10.1002/2016GL070067

693 Kay, J. E., Deser, C., Phillips, A., Mai, A., Hannay, C., Strand, G., Arblaster, J., Bates, S.,  
694 Danabasoglu, G., Edwards, J., Holland, M. Kushner, P., Lamarque, J.-F., Lawrence, D.,  
695 Lindsay, K., Middleton, A., Munoz, E., Neale, R., Oleson, K., Polvani, L., & Vertenstein,  
696 M. (2015), The Community Earth System Model (CESM) Large Ensemble Project: A  
697 Community Resource for Studying Climate Change in the Presence of Internal Climate  
698 Variability, *Bulletin of the American Meteorological Society*, 96, 1333–1349.  
699 doi:10.1175/BAMS-D-13-00255.1.

700 Kay, J. E., Holland, M. M., & Jahn, A. (2011), Inter-annual to multi-decadal Arctic sea ice extent  
701 trends in a warming world. *Geophysical Research Letters*, 38, L15708.  
702 <https://doi.org/10.1029/2011GL048008>

703 Kirchmeier-Young, M. C., F. W. Zwiers, & Gillett, N. P. (2017), Attribution of extreme events  
704 in Arctic sea ice extent, *J. Clim.*, 30, 553–571 doi:10.1175/JCLI-D-16-0412.1.

705 Latif, M., T. Martin, & Park, W. (2013), Southern Ocean sector centennial climate variability and  
706 recent decadal trends, *J. Clim.*, 26(19), 7767–7782.

707 Mahlstein, I., & Knutti, R. (2012), September Arctic sea ice predicted to disappear near 2°C  
708 global warming above present, *J. Geophys. Res.*, 117, D06104,  
709 doi:10.1029/2011JD016709.

710 Massonnet, F., Vancoppenolle, M., Goosse, H., Docquier, D., Fichefet, T., & Blanchard-  
711 Wrigglesworth, E. (2018), Arctic sea-ice change tied to its mean state through  
712 thermodynamic processes. *Nature Climate Change*, 8(7), 599–603.  
713 <https://doi.org/10.1038/s41558-018-0204-z>

714 Mauritsen, T., Stevens, B., Roeckner, E., Crueger, T., Esch, M., Giorgetta, M., Haak, H.,  
715 Jungclaus, J., Klocke, D., Matei, D., Mikolajewicz, U. Notz, D., Pincus, R., Schmidt, H., &  
716 L. Tomassini (2012), Tuning the climate of a global model. *Journal of Advances in*  
717 *Modeling Earth Systems*, 4, M00A01. <https://doi.org/10.1029/2012MS000154>

718 Mioduszewski, J., S. Vavrus, M. Wang, M. Holland, & Landrum, L. (2019), Past and future  
719 interannual variability in Arctic sea ice in coupled climate model. *Cryosphere*, 13, 113–  
720 124, <https://doi.org/10.5194/tc-13-113-2019>.

721 Notz, D. (2015), How well must climate models agree with observations? *Philosophical*  
722 *Transactions of the Royal Society A*, 373(2052), 20140164.  
723 <https://doi.org/10.1098/rsta.2014.0164>

724 O'Neill, B. C., Tebaldi, C., van Vuuren, D. P., Eyring, V., Friedlingstein, P., Hurtt, G., Knutti, R.,  
725 Kriegler, E., Lamarque, J.-F., Lowe, J., Meehl, G. A., Moss, R., Riahi, K., & Sanderson, B.  
726 M. (2016), The Scenario Model Intercomparison Project (ScenarioMIP) for CMIP6,  
727 *Geosci. Model Dev.*, 9, 3461–3482, <https://doi.org/10.5194/gmd-9-3461-2016>.

728 Phillips, A. S., C. Deser, J. Fasullo, D. P. Schneider & Simpson, I. R. (2020), Assessing Climate  
729 Variability and Change in Model Large Ensembles: A User's Guide to the "Climate  
730 Variability Diagnostics Package for Large Ensembles", doi:10.5065/h7c7-f961

731 Roach, L. A., Dörr, J., Holmes, C. R., Massonnet, F., Blockley, E. W., Notz, D., & Bitz, C.  
732 M. (2020), Antarctic sea ice in CMIP6. *Geophysical Research Letters*, 47,  
733 e2019GL086729. <https://doi.org/10.1029/2019GL086729>

734 Rodgers, K., Lee, S-S., Rosenbloom, N., Timmerman, A., Danabasoglu, G., Deser, C., Edwards,  
735 J., Kim, J-E., Simpson, I., Stein, K, Stuecker, M., F., Yamaguchi, R., Bodai, T., Chang, E-  
736 S., Huang, L., Kim, W. M., Lamarque, J.-F., Lombardozzi, D., Wieder, W. R., & S. G.  
737 Yeager (2021), Ubiquity of human-induced changes in climate variability, *Earth Syst.*  
738 *Dynam. Discuss*, accepted, <https://doi.org/10.5194/esd-2021-50>.

739 Rohde, R. A. and Hausfather, Z., 2020. The Berkeley Earth Land/Ocean Temperature Record,  
740 *Earth Syst. Sci. Data*, 12, 3469-3479, <https://doi.org/10.5194/essd-12-3469-2020>.

741 Rosenblum, E. & Eisenman, I. (2017), Sea ice trends in climate models only accurate in runs  
742 with biased global warming. *Journal of Climate*, 30(16), pp.6265-6278.

743 Sigmond, M., Fyfe, J. C. & N. C. Swart (2018), Ice-free Arctic projections under the Paris  
744 Agreement, *Nat. Clim. Change*, [https://doi.org/10.1038/s41558-018-](https://doi.org/10.1038/s41558-018-0124-y)  
745 0124-y (2018)

746 Notz, D. & SIMIP Community (2020), Arctic Sea Ice in CMIP6, *Geophysical Research Letters*,  
747 47(10), e2019GL086749. doi:10.1029/2019GL086749

748 Singh, H. K. A., Landrum, L., Holland, M. M., Bailey, D. A., & DuVivier, A. K. (2021), An overview  
749 of Antarctic sea ice in the Community Earth System Model version 2, part I: Analysis of  
750 the seasonal cycle in the context of sea ice thermodynamics and coupled atmosphere-  
751 ocean-ice processes. *Journal Of Advances In Modeling Earth Systems*, 13,  
752 e2020MS002143. doi:10.1029/2020MS002143

753 Smith, D. M., R. Eade, M. Andrews, H. Ayres, A. Clark, S. Chripko, C. Deser, N. J. Dunstone, J.  
754 Garcia-Serrano, G. Gastineau, L. S. Graff, S. C. Hardiman, B. He, L. Hermanson, T. Jung,  
755 J. Knight, X. Levine, G. Magnusdottir, E. Manzini, D. Matei, M. Mori, R. Msadek, P. Ortega,  
756 Y. Peings, A. A. Scaife<sup>1</sup>, J. A. Screen, M. Seabrook, T. Semmler, M. Sigmond, J. Streffing,  
757 L. Sun, and A. Walsh (2021), Robust but weak winter atmospheric circulation response to  
758 future Arctic sea ice loss. *Nat. Comm.*, in press.

759 Swart, N. C., Fyfe, J. C., Hawkins, E., Kay, J. E., & Jahn, A. (2015), Influence of internal  
760 variability on Arctic sea-ice trends, *Nature Climate Change*, 5, 86-89,  
761 doi:10.1038/nclimate2483.

762 Taylor, K. E., R. J. Stouffer, & Meehl, G. A. (2012), The CMIP5 experiment design, *Bull. Am.*  
763 *Meteorol. Soc.*, 93, 485–498, doi:10.1175/BAMS-D-11-00094.1.

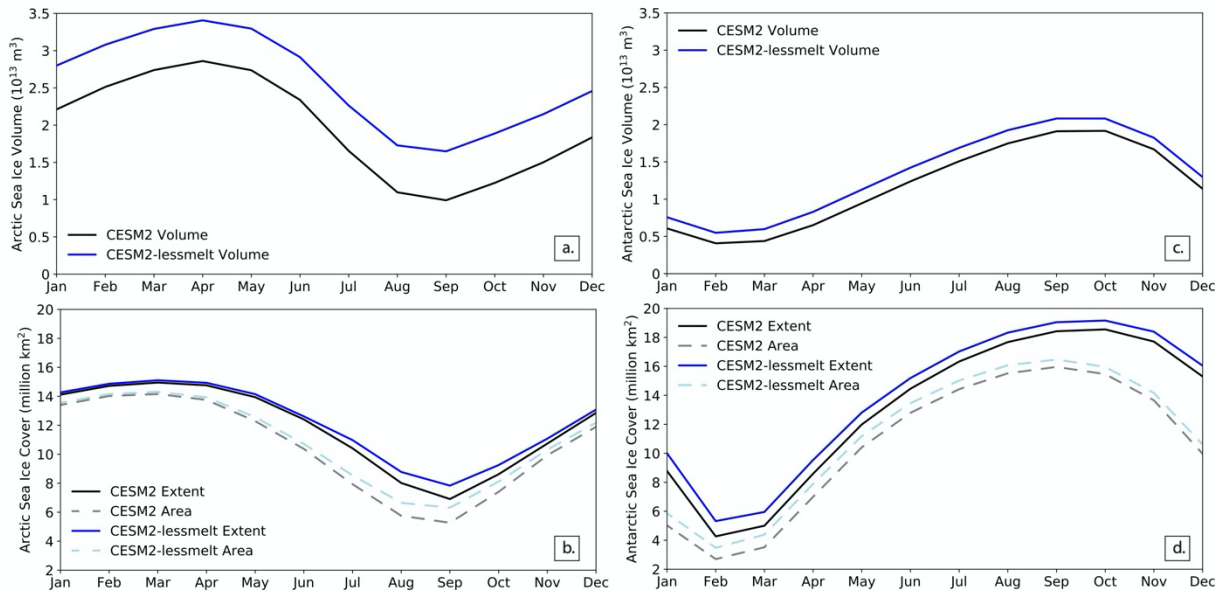
764 Webster, M. A., DuVivier, A. K., Holland, M. M., & Bailey, D. A. (2021), Snow on Arctic sea ice in  
765 a warming climate as simulated in CESM. *Journal Of Geophysical Research: Oceans*,  
766 126, e2020JC016308. doi:10.1029/2020JC016308

767 Wettstein, J. J. & Deser, C. (2014), Internal variability in projections of twenty-first century Arctic  
768 sea ice loss: Role of the large-scale atmospheric circulation. *J. Climate*, 27, 527-550, doi:  
769 10.1175/JCLI-D-12-00839.1.

770 Yeager, S., Karspeck, A., & Danabasoglu, G. (2015), Predicted slowdown in the rate of Atlantic  
771 sea ice loss. *Geophysical Research Letters*, 42, 10704-10713.  
772 doi:10.1002/2015GL065364

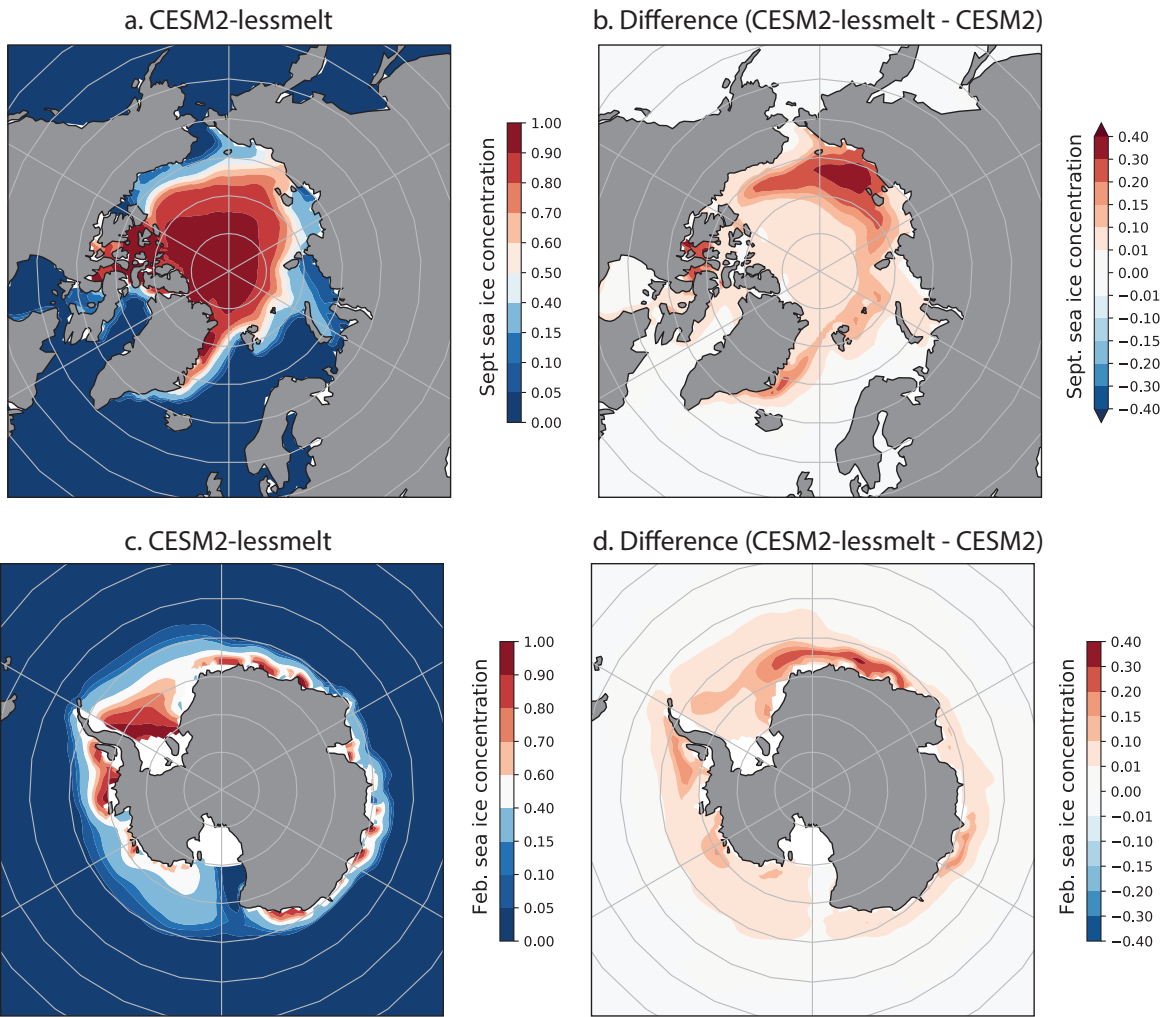


774 **Figures**  
775  
776

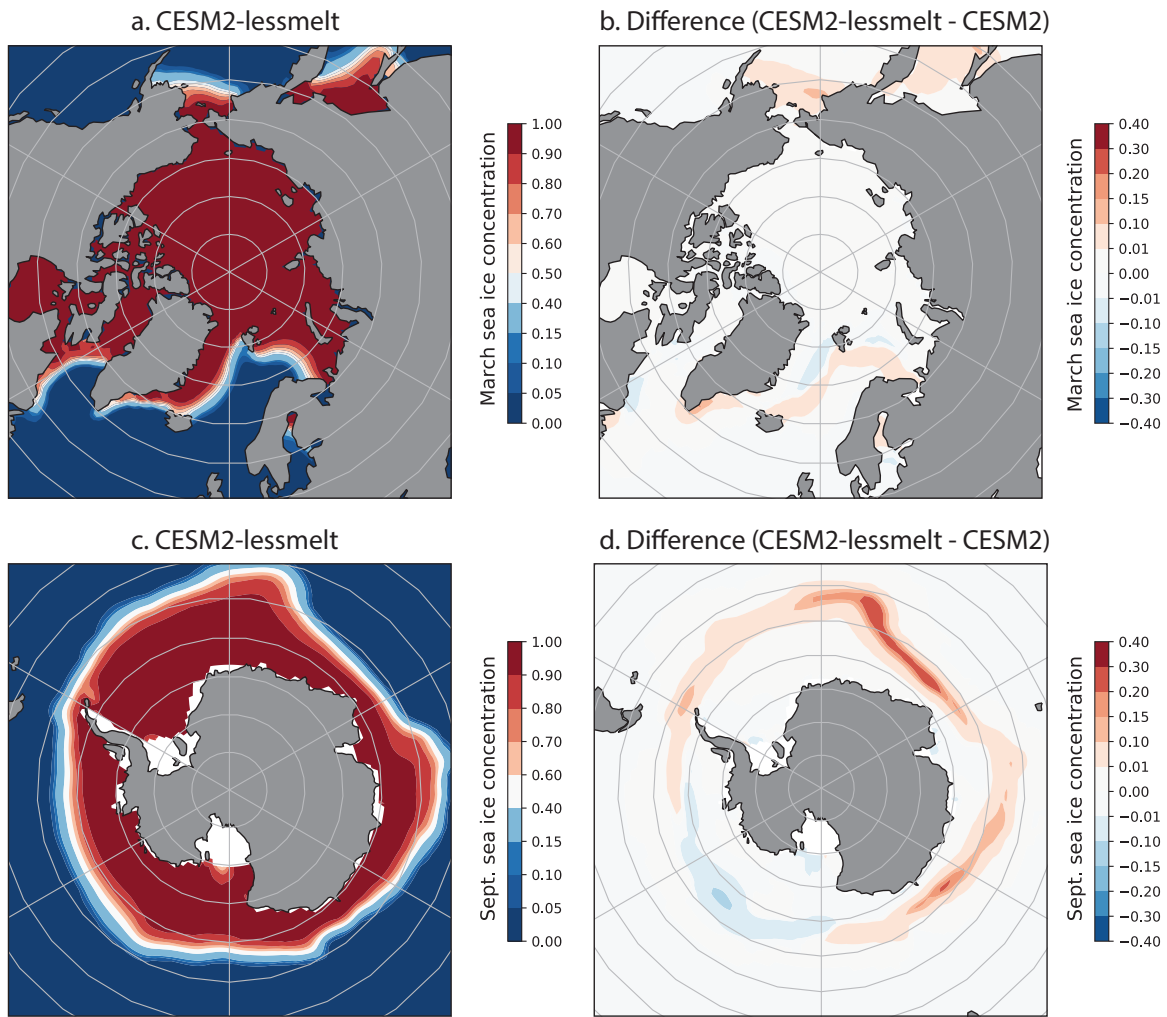


777 **Figure 1.** Seasonal cycle in CESM2 and CESM2-lessmelt 1850 preindustrial control runs: a) Arctic  
778 sea ice volume, b) Arctic sea ice area and extent, c) Antarctic sea ice volume, d) Antarctic sea ice  
779 area and extent. Values are overlapping 200-year averages (years 911-1110 of the CESM2  
780 CMIP6 1850 pre-industrial control run).  
781

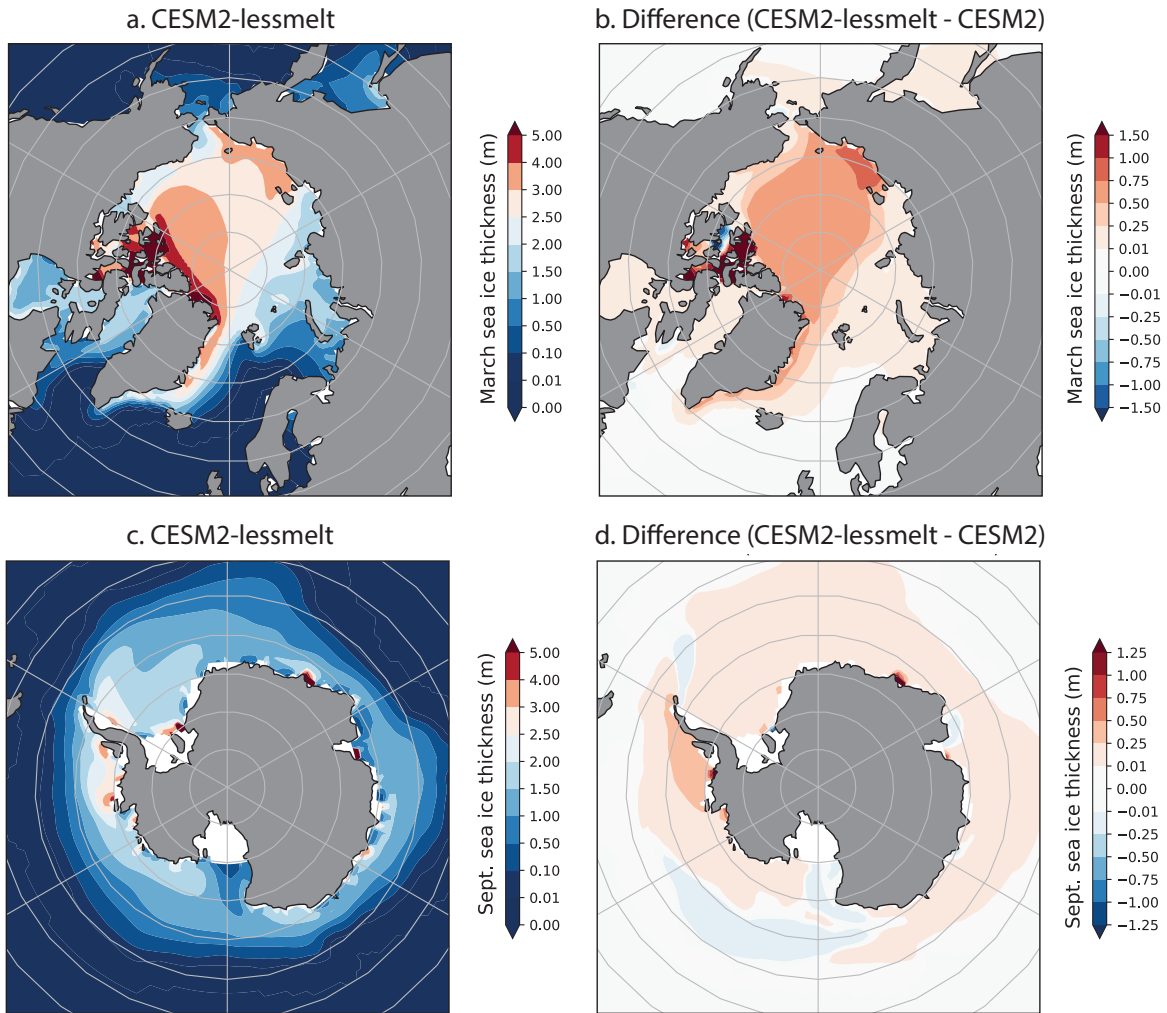
782  
783



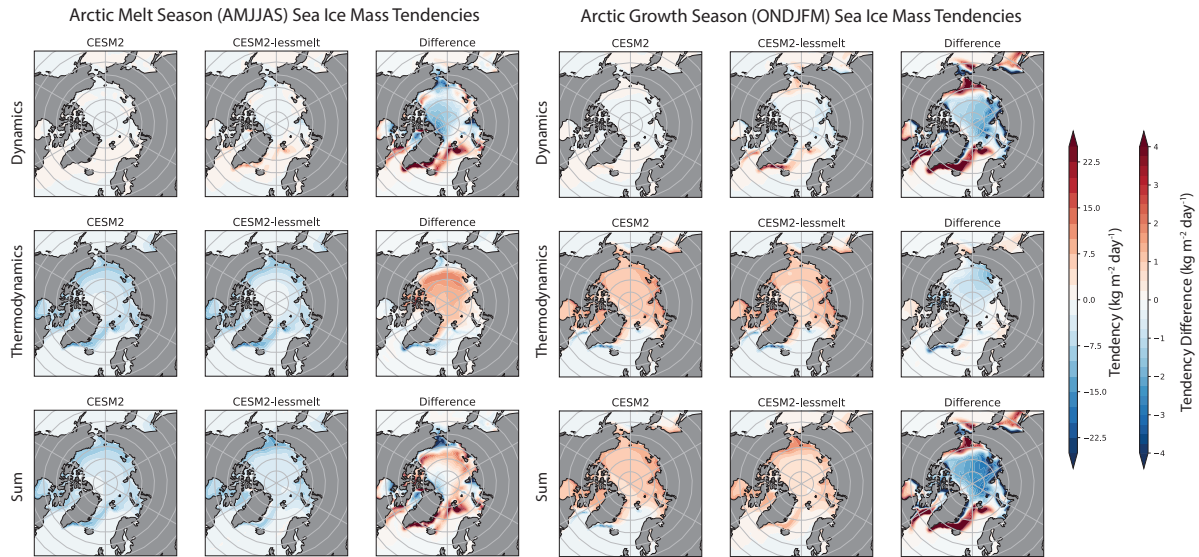
784  
 785 **Figure 2.** Late summer sea ice concentration in preindustrial control runs: a) September Arctic  
 786 CISM2-lessmelt, b) Difference September Arctic (CESM2-lessmelt - CESM2), c) February  
 787 Antarctic CISM2-lessmelt, d) Difference February Antarctic (CESM2-lessmelt - CESM2). Values  
 788 are overlapping 200-year averages as in Figure 1. *Note: Nonlinear color scale used to emphasize*  
 789 *low ice concentrations.*  
 790



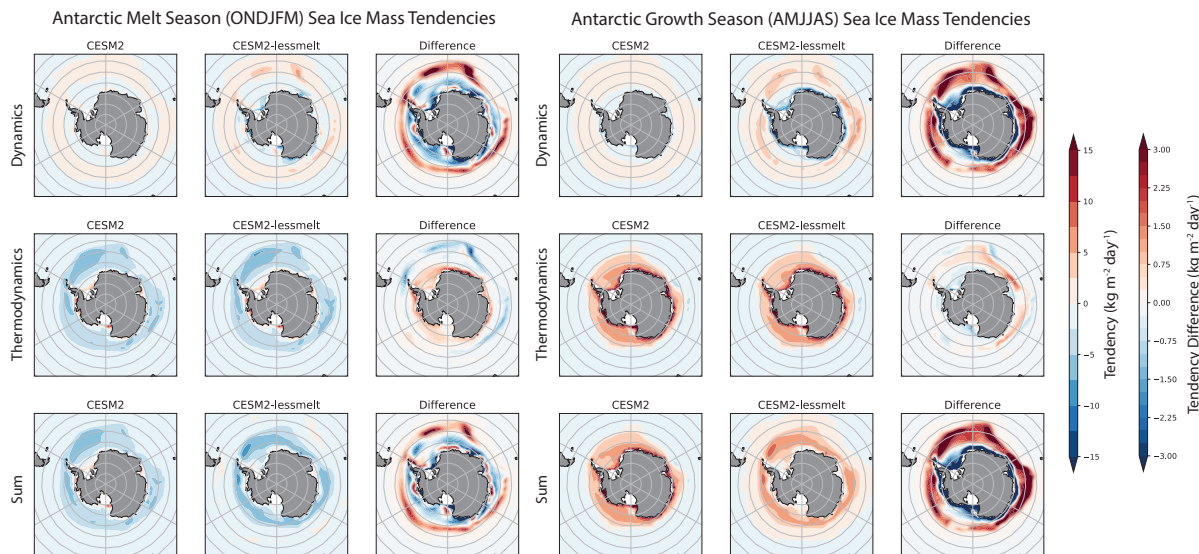
791  
 792 **Figure 3.** Late winter sea ice concentration in preindustrial control runs: a) CESM2-tuned ice  
 793 March Arctic, b) Difference March Arctic, c) CESM2-lessmelt September Antarctic, d) Difference  
 794 September Antarctic. Values are overlapping 200-year averages as in Figure 1. *Note: Nonlinear*  
 795 *color scale used to emphasize low ice concentrations.*  
 796



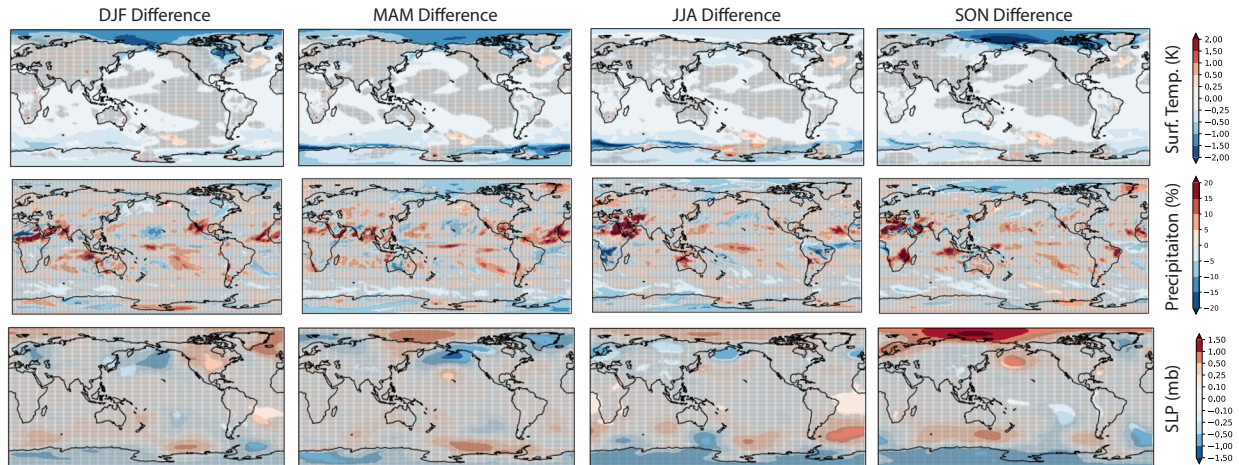
797  
 798 **Figure 4.** Late winter sea ice thickness in preindustrial control runs: a) CESM2 March Arctic, b)  
 799 CESM2-lessmelt March Arctic, c) CESM2 September Antarctic, d) CESM2-lessmelt September  
 800 Antarctic. Values are overlapping 200-year averages as in Figure 1. *Note: Nonlinear color scale*  
 801 *used to emphasize thin ice categories.*  
 802



803  
 804 **Figure 5. Arctic sea ice mass tendency terms for the melt season [AMJJAS] (left), and the**  
 805 **growth season [ONDJFM] (right).** For each season, the top row is tendency due to dynamics  
 806 (sidmassdyn), the middle row is tendency due to thermodynamics (sidmassth), and the bottom  
 807 row is their sum. All differences are CESM2-lessmelt minus CESM2. Values are overlapping 200-  
 808 year averages as in Figure 1.  
 809

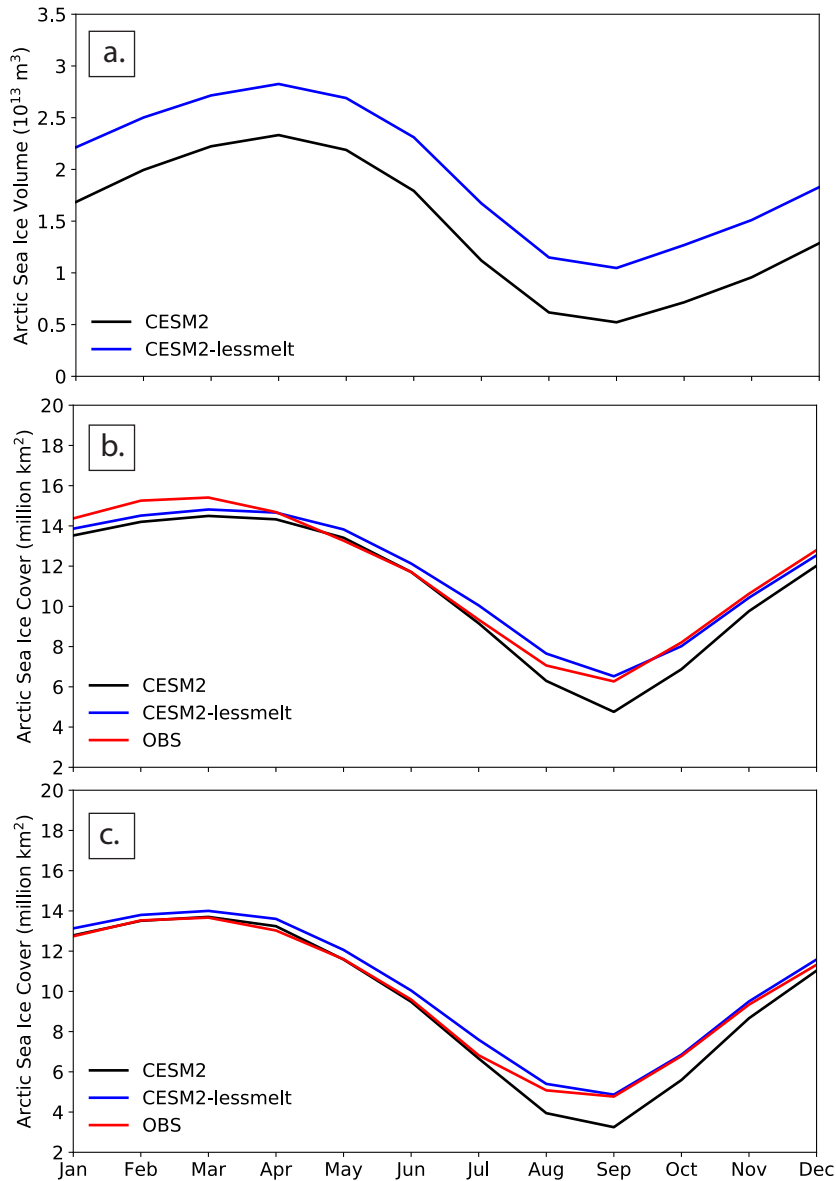


810  
 811 **Figure 6. Antarctic sea ice mass tendency terms for the melt season [ONDJFM] (left), and the**  
 812 **growth season [AMJJAS] (right).** For each season, the top row is tendency due to dynamics  
 813 (sidmassdyn), the middle row is tendency due to thermodynamics (sidmassth), and the bottom  
 814 row is their sum. All differences are CESM2-lessmelt minus CESM2. Values are overlapping 200-  
 815 year averages as in Figure 1.  
 816

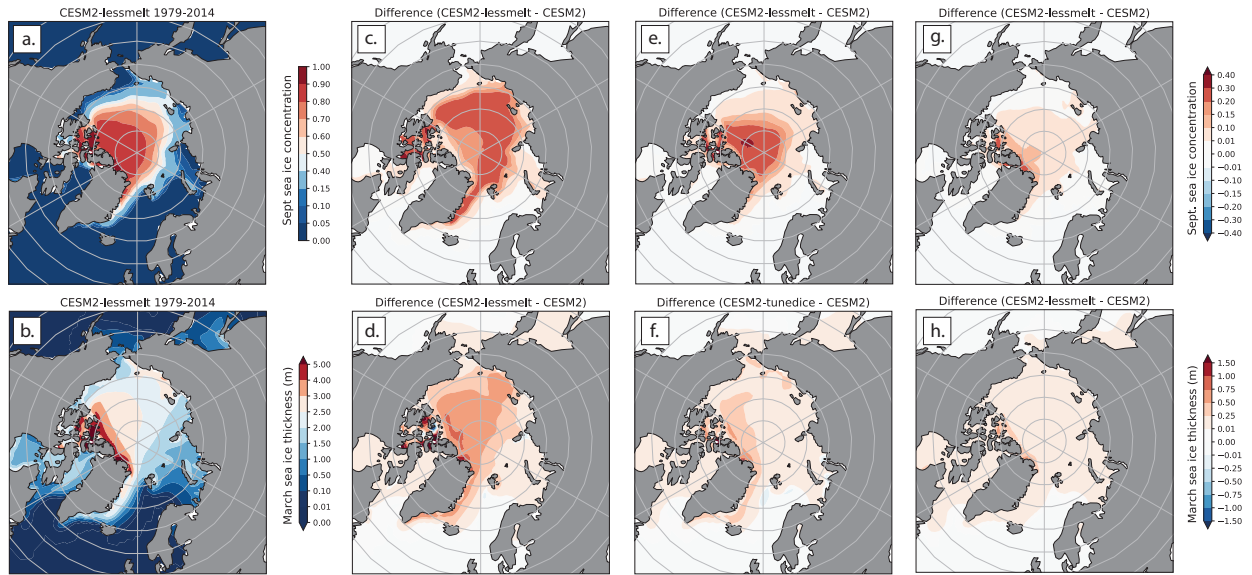


817  
818  
819  
820  
821  
822  
823

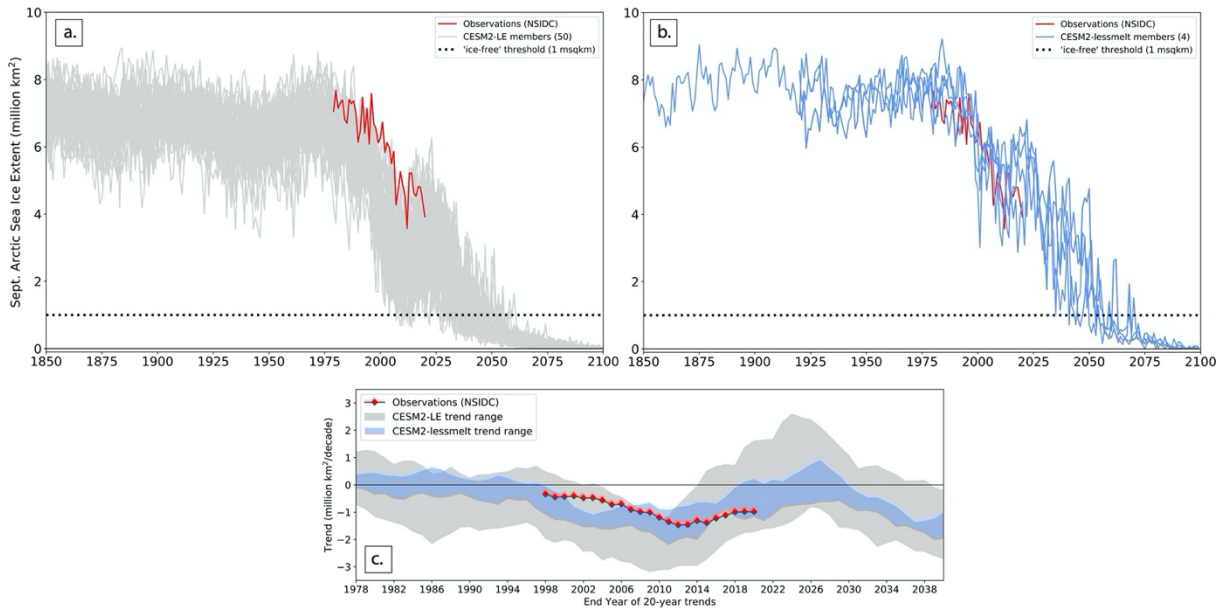
**Figure 7. Global maps of pre-industrial control differences (CESM2-lessmelt minus CESM2) by season.** Top row shows surface temperature (K). Middle row shows total precipitation (% difference). Bottom row shows sea level pressure (mb). Grey stippling shows regions that are not statistically different at the 95% confidence level using a 2-sided t-test. Values are overlapping 200-year averages as in Figure 1.



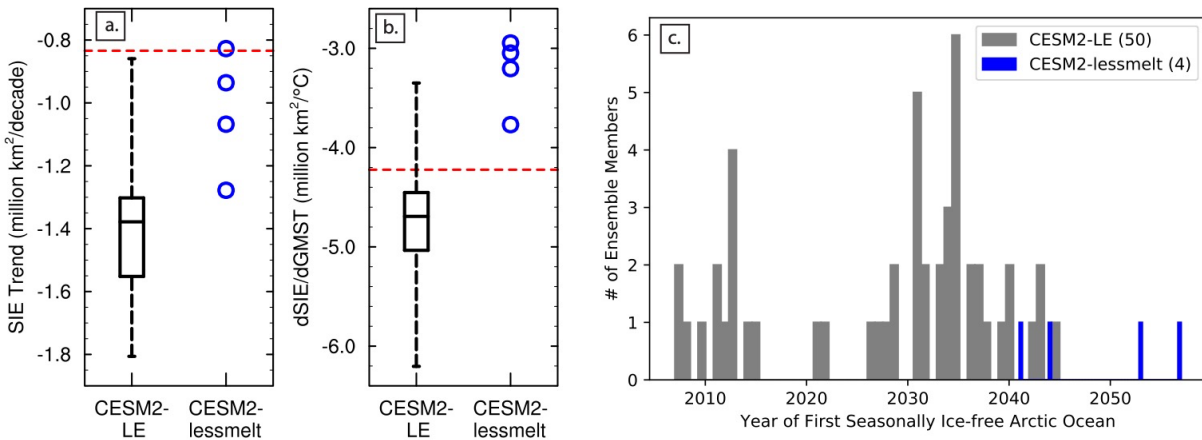
824  
 825 **Figure 8. Present-day (1979-2014) ensemble mean seasonal cycle in CESM2-LE and CESM2-**  
 826 **lessmelt: a) Arctic sea ice volume, b) Arctic sea ice extent, c) Arctic sea ice area. Observations**  
 827 **are from NSIDC sea ice index with pole filling (Fetterer et al. 2017).**  
 828



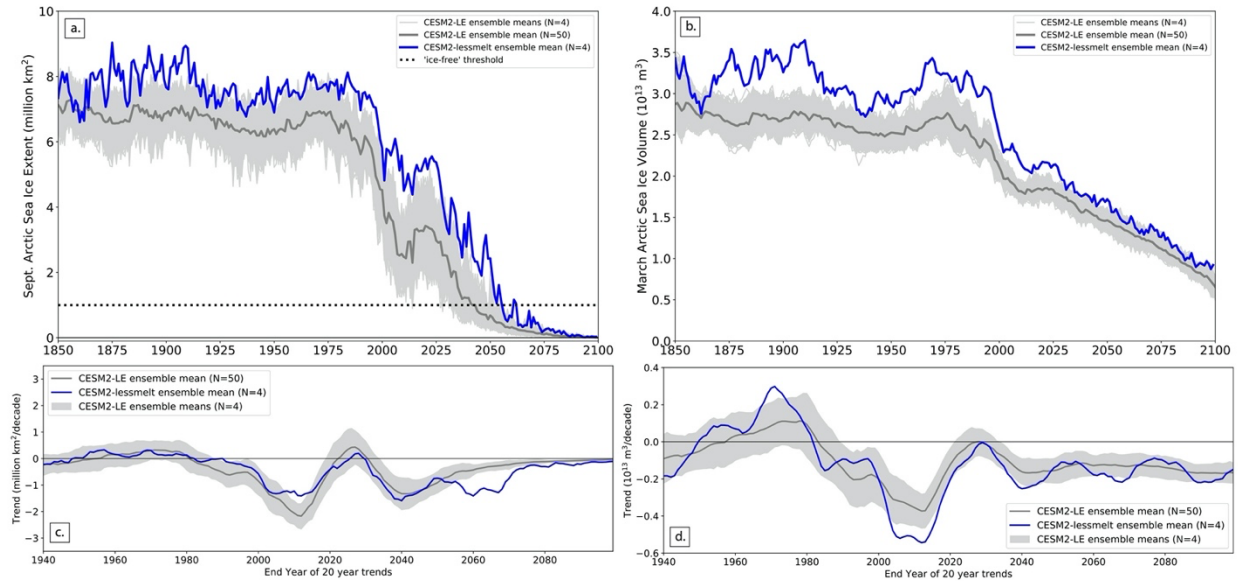
829  
 830 **Figure 9. Ensemble mean Arctic sea ice maps: a) Present-day (1979-2014) CSM2-lessmelt**  
 831 **September concentration, b) as in a) but for March thickness, c-d) as in a-b) but for the**  
 832 **CSM2-lessmelt minus CSM2-LE difference, e-f) as in c-d) but for 2030-2049, g-h) as in c-d)**  
 833 **but for 2050-2069**  
 834  
 835



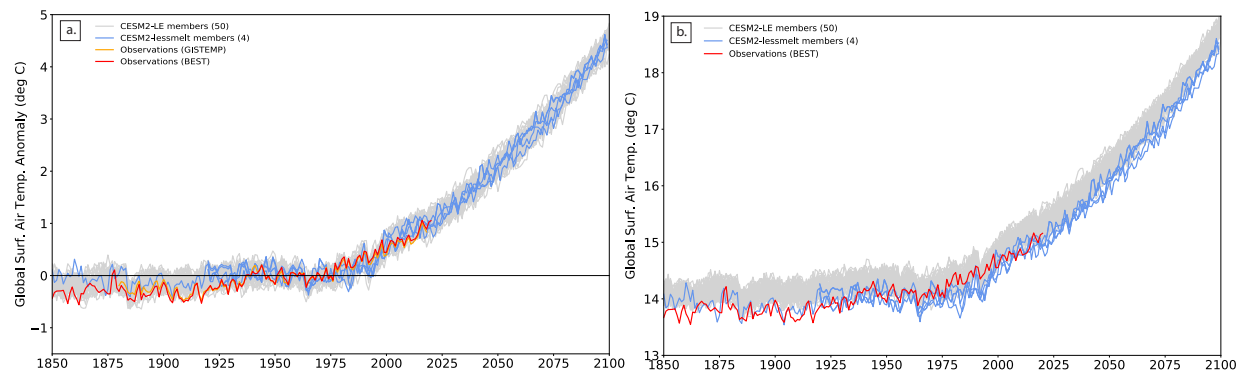
836  
 837 **Figure 10. Arctic September sea ice extent transient evolution: a) CESM2-LE 1850-2100**  
 838 **timeseries, b) CESM2-lessmelt 1850-2100 timeseries, c) 20-year trends in CESM2-LE, CESM2-**  
 839 **lessmelt, and observations with end years of 1999-2049.** Observations are from NSIDC sea ice  
 840 index (Fetterer et al. 2017) with area pole-filling.  
 841  
 842



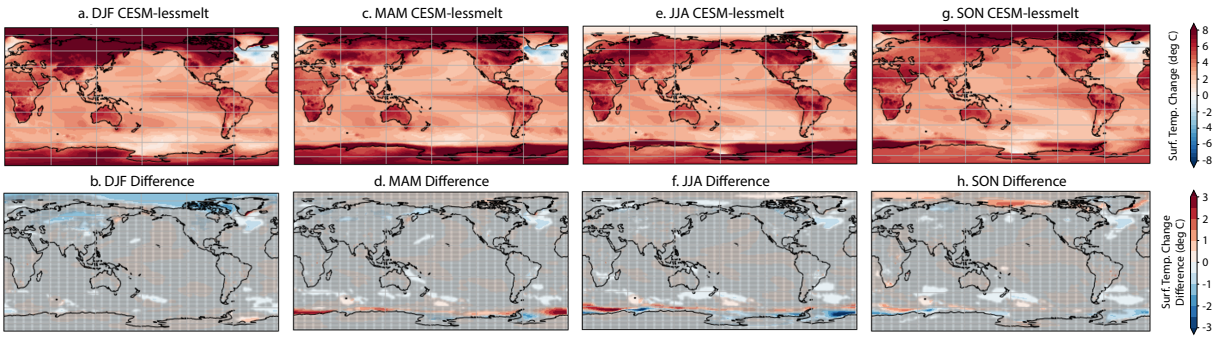
843  
 844 **Figure 11. Arctic sea ice comparison metrics: a) September sea ice trends, b) sea ice sensitivity**  
 845 **defined as the change in September sea ice extent per degree of change in global mean**  
 846 **surface temperature (dSIE/dGMST), and c) year of first seasonally ice-free Arctic Ocean.** Sea  
 847 ice extent trend and sensitivity calculations follow protocol and years (1979-2014) used for  
 848 evaluation of CMIP6 by SIMIP Community (2020). In a) and b), the observations are shown as a  
 849 red dashed line and the CESM2 Large Ensemble is shown as a box indicating the interquartile  
 850 range, a line inside the box indicating the median, and whiskers to show the minimum and  
 851 maximum across all ensemble members. In c), a seasonally ice-free Arctic Ocean occurs when  
 852 the September sea ice extent first falls below 1 million sq. km.  
 853



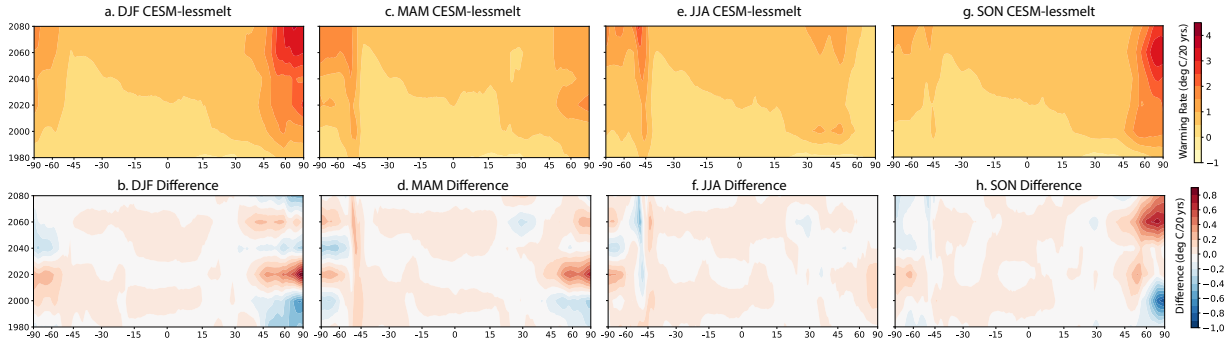
854  
 855 **Figure 12. CSM2-LE and CSM2-lessmelt Arctic sea ice: a) September extent ensemble mean**  
 856 **1850-2100 timeseries, b) March volume ensemble mean 1850-2100 timeseries, c) September**  
 857 **extent ensemble mean 20-year trends, d) March volume ensemble mean trends.** Grey shading  
 858 shows 95% confidence intervals on trends calculated by bootstrapping CSM2-LE ensemble  
 859 means with 4 members 1,000 times.  
 860



861  
 862 **Figure 13. Transient evolution global annual mean surface air temperature in CSM2-LE and**  
 863 **CSM2-lessmelt: a) anomaly from 1951-1980, b) absolute value.** Observations are from  
 864 GISTEMP (Hansen et al. 2010) and BEST (Rohde and Hausfather, 2020).  
 865  
 866



867  
 868 **Figure 14. Ensemble mean surface temperature change (2080-2099 minus 1920-1939) by**  
 869 **season: a) DJF CESM2-lessmelt, b) DJF Difference (CESM2-lessmelt minus CESM2-LE), c-d) as in**  
 870 **a-b) but for MAM, e-f) as in a-b) but for JJA, c-d) as in g-h) but for SON. Stippling on difference**  
 871 **maps indicates where differences between CESM2-lessmelt and CESM2-LE ensemble means are**  
 872 **\*not\* statistically significant at the 95% confidence level.**  
 873



874  
 875 **Figure 15. Zonal ensemble mean surface warming rate (deg C/20 years) by season: a) DJF**  
 876 **CESM2-lessmelt, b) DJF difference (CESM2-lessmelt minus CESM2-LE), c-d) as in a-b) but for**  
 877 **MAM, e-f) as in a-b) but for JJA, c-d) as in g-h) but for SON. Warming rates are calculated using**  
 878 **20 years and the start year plotted on the vertical axis.**